

1.1 VAPOUR COMPRESSION REFRIGERATION SYSTEM

The ideal vapor-compression cycle uses refrigerant as the working fluid to absorb and reject heat energy. The energy transfer allows the vapor-compression cycle to reduce or cool a closed environment. The ideal vapor-compression cycles assumes that the system is perfect based on thermodynamic theory, therefore neglecting any losses associated to performance.

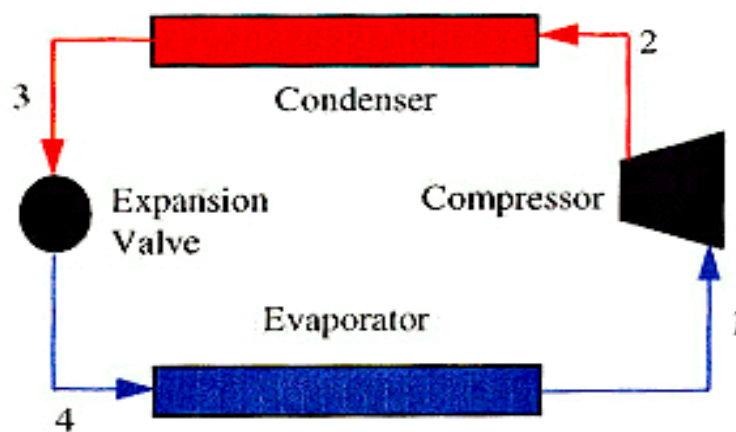


Fig1.1 Typical vapor compressionrefrigeration cycle diagram.

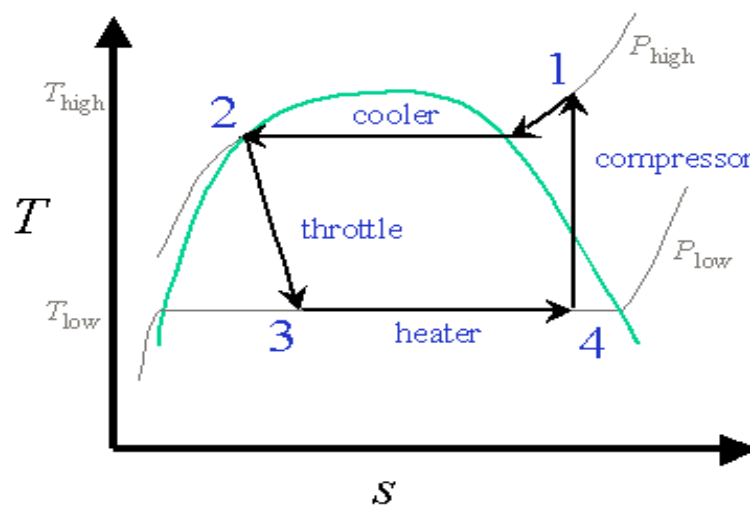


Fig1.2. T-s Diagram

In the ideal vapor-compression cycle, refrigerant enters the compressor as a saturated vapor (Figure 1.1). As the refrigerant is compressed, it increases in temperature and pressure (points 1-2). After the compressor the refrigerant passes through the condenser. Heat energy (Q_h) is exchanged with the surrounding environment causing the refrigerant to cool and become a saturated liquid (points 2-3). Next, the refrigerant passes through the expansion valve causing the temperature and pressure to decrease (points 3-4). Because of the reduction in temperature and pressure, the refrigerant enters the evaporator as a saturated mixture. As the refrigerant passes through the evaporator, it absorbs heat energy (Q_L) from the environment that it is trying to cool. The refrigerant exits the evaporator as a saturated vapor and returns to the compressor to begin the process all over again (points 4-1).

Due to fluid friction, heat transfer losses, and component inefficiency, the refrigeration cycle is unable to achieve complete thermodynamic saturation. The result of the inefficiencies and losses prevent the refrigeration cycle from operating at the optimum performance. This is called the actual vapor-compression refrigeration cycle.

When designing a refrigeration system, it is important to understand how the refrigeration cycle works and the effects of component inefficiency on overall performance. Another important factor when designing a refrigeration system is the working fluid. The working fluid is commonly referred to as refrigerant. It is the media used to absorb and reject heat energy. Chlorofluorocarbons (CFCs), ammonia, propane, ethane, ethylene, carbon dioxide, air and water are just some of the refrigerants used in refrigeration systems. The design of the system should include refrigerant that is nontoxic, noncorrosive, nonflammable, chemically stable, and inexpensive.

1.2 VAPOUR ABSORPTION REFRIGERATION SYSTEM

The function of the compressor in the vapour compression system is to continuously withdraw the refrigerant vapour from the evaporator and to raise its pressure and hence temperature, so that the heat absorbed in the evaporator, along with the work of compression, may be rejected in the condenser to the surroundings.

In the vapour absorption system, the function of the compressor is accomplished in a three step process by the use of absorber, pump and generator or reboiler as follows:

- i. *Absorber*: Absorption of the refrigerant vapour by its weak or poor solution in a suitable absorbent or adsorbent, forming a strong or rich solution of the refrigerant in the absorbent/adsorbent.
- ii. *Pump*: Pumping of the rich solution raising its pressure to the condenser pressure.
- iii. *Generator or Desorber*: Distillation of the vapour from the rich solution leaving the poor solution for recycling.

A simple vapour-absorption system, therefore consists of a condenser, an expansion device and an evaporator as in the vapour compression system, and in addition, an absorber, a pump, a generator and a pressure reducing valve to replace the compressor.

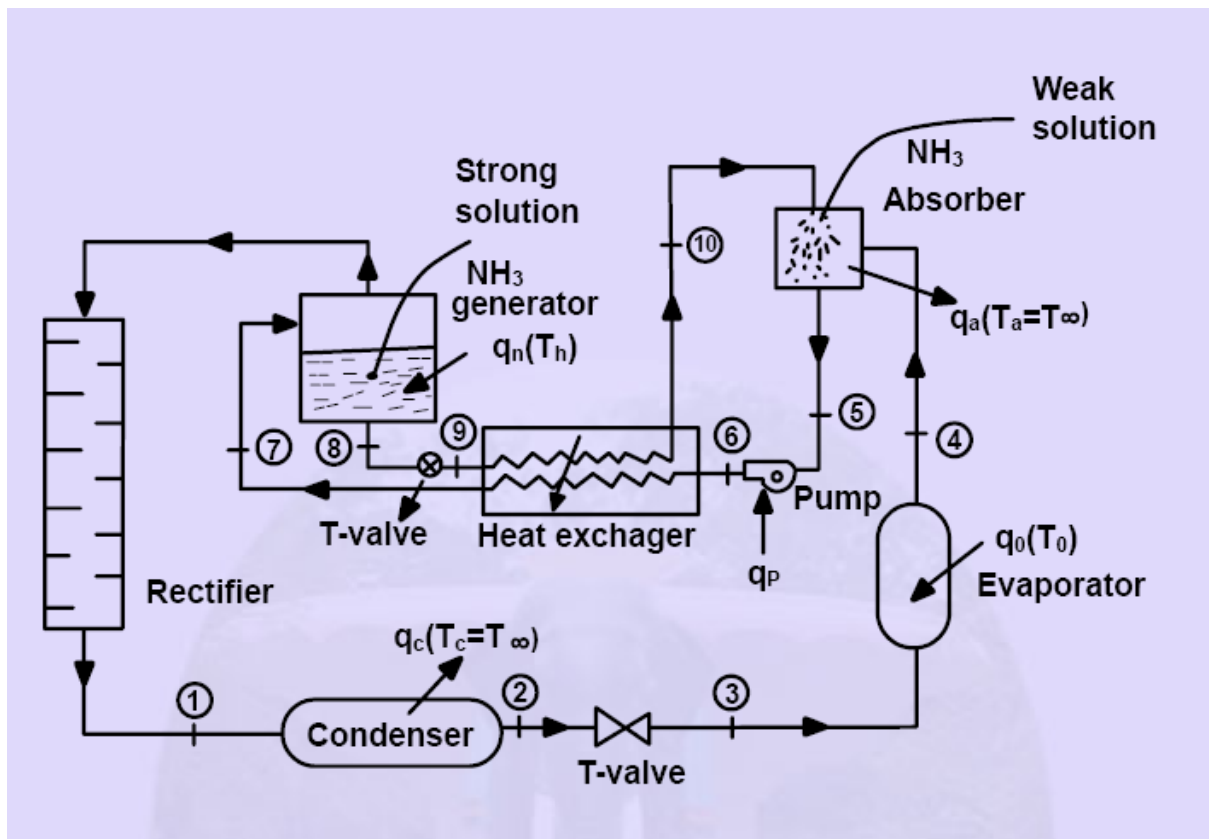


Fig 1.3 Vapour Absorption system

Some liquids like water have great affinity for absorbing large quantities of certain vapours (NH_3) and reduce the total volume greatly. The absorption refrigeration system differs fundamentally from vapour compression system only in the method of compressing the refrigerant. An absorber, generator and pump in the absorption refrigerating system replace the compressor of a vapour compression system. Figure 1.3 shows the schematic diagram of a vapour absorption system. Ammonia vapour is produced in the generator at high pressure from the strong solution of NH_3 by an external heating source. The water vapour carried with ammonia is removed in the rectifier and only the dehydrated ammonia gas enters into the condenser. High pressure NH_3 vapour is condensed in the condenser. The cooled NH_3 solution is passed through a throttle valve and the pressure and temperature of the refrigerant are reduced below the temperature to be maintained in the evaporator. The low temperature refrigerant enters the evaporator and absorbs the required heat from the evaporator and leaves the evaporator as saturated vapour. Slightly superheated, low pressure NH_3 vapour is absorbed by the weak solution of NH_3 which is sprayed in the absorber as shown in Fig.1.1. Weak NH_3 solution (aqua-ammonia) entering the absorber becomes strong solution after absorbing NH_3 vapour and then it is pumped to the generator through the heat exchanger. The pump increases the pressure of the strong solution to generator pressure. The strong NH_3 solution coming from the absorber absorbs heat from high temperature weak NH_3 solution in the heat exchanger. The solution in the generator becomes weak as NH_3 vapour comes out of it. The weak high temperature ammonia solution from the generator is passed to the heat exchanger through the throttle valve. The pressure of the liquid is reduced to the absorber pressure by the throttle valve.

1.3 COMPARISON BETWEEN VAPOUR COMPRESSION AND ABSORPTION SYSTEM

Absorption system	Compression System
a) Uses low grade energy like heat. Therefore, may be worked on exhaust systems from I.C engines, etc.	a) Using high-grade energy like mechanical work.
b) Moving parts are only in the pump, which is a small element of the system. Hence operation is smooth.	b) Moving parts are in the compressor. Therefore, more wear, tear and noise.
c) The system can work on lower evaporator pressures also without affecting the COP.	c) The COP decreases considerably with decrease in evaporator pressure
d) No effect of reducing the load on performance.	d) Performance is adversely affected at partial loads.
e) Liquid traces of refrigerant present in piping at the exit of evaporator constitute no danger.	e) Liquid traces in suction line may damage the compressor.
f) Automatic operation for controlling the capacity is easy.	f) It is difficult.

1.4 PRINCIPLES OF VAPOUR ABSORPTION SYSTEM

Absorptive refrigeration uses a source of heat to provide the energy needed to drive the cooling process.

The absorption cooling cycle can be described in three phases:

1. Evaporation: A liquid refrigerant evaporates in a low partial pressure environment, thus extracting heat from its surroundings – the refrigerator.
2. Absorption: The gaseous refrigerant is absorbed – dissolved into another liquid - reducing its partial pressure in the evaporator and allowing more liquid to evaporate.

3. Regeneration: The refrigerant-laden liquid is heated, causing the refrigerant to evaporate out. It is then condensed through a heat exchanger to replenish the supply of liquid refrigerant in the evaporator.

1.5 COMMON REFRIGERANT –ABSORBENT SYSTEMS

Thermodynamic requirements of the mixture are:

- I. *Solubility Requirement*: The refrigerant should have more than Raoult's law solubility in the absorbent or adsorbent so that a strong solution, highly rich in the refrigerant, is formed in the absorber by the absorption of the refrigerant vapour.
- II. *Boiling Point Requirement*: There should be a large difference in the normal boiling points of the two substances, at least 200 °C, so that the absorbent exerts negligible vapour pressure at the generator temperature. Thus almost absorbent-free refrigerant is boiled off from the generator and the absorbent alone returns to the absorber. If absorbent vapour goes with the refrigerant vapour to the refrigerant circuit, the refrigeration produced will not be isothermal. In case a solid adsorbent is used, it does not exert any vapour pressure. Thus, pure refrigerant vapour only will go to the refrigerant circuit.

The two commonly used pairs are those of refrigerant NH_3 + absorbent H_2O , and Refrigerant H_2O + adsorbent LiBr_2 .

In the ammonia –water system, ammonia is the refrigerant and water is the absorbent. Ammonia forms a highly non ideal solution in water. Hence from the point of view of the solubility requirement it is satisfactory. But the difference in their boiling points is only 138 °C. Hence the vapour leaving the generator contains some amount of water.

Thus the ammonia-water system is not suitable from the point of view of the boiling point requirement.

In the water lithium bromide system, water is the refrigerant and the lithium bromide is the adsorbent. Hence the mixture is used only in air conditioning applications since water freezes at 0°C. The mixture is again non ideal and is satisfactory from the point of view of the solubility requirement. Since lithium bromide is a salt, it exerts no vapour pressure. So vapour leaving the generator is a pure refrigerant. The mixture, therefore satisfies the boiling point requirement also.

1.6 DESIRABLE PROPERTIES OF A PRIMARY REFRIGERANT

1. The liquid has to vaporise at the evaporator coil to cause cooling. The liquid at the evaporator coil should therefore vaporise easily, otherwise the compressor will have to create too much of vacuum to cause the liquid to vaporise. **Thus, 'Boiling Point' of the refrigerant should be low.**
2. Pressure to which compressor has to compress the drawn gases, to convert them back into liquid at the condenser, should be low. **Therefore the refrigerant vapours should be easily condensable.**
3. Every kilogram of liquid refrigerant vaporised at the evaporator coil should take away a large amount of heat, i.e. **'Specific Enthalpy of Vaporisation' (latent heat) of refrigerant should be high. Otherwise mass flow rate will be high.**
4. Once the evaporated gas is compressed, the temperature of seawater should be low enough (below critical temperature of the refrigerant) to be able to condense these gases to liquid form. **Thus 'Critical Temperature' of the refrigerant should be high.**
5. Vapour produced after vaporisation of the liquid at the evaporator coil should occupy minimum volume, to keep pipeline diameter, compressor size, etc. small and compact. **Thus refrigerant vapour should have low 'Specific Volume'.**
6. **Non-Corrosive**
7. **Stable**
8. **Non-flammable and Non-explosive**
9. **Compatible with crank case oil, oil seals, gaskets, metal involved, etc.**
10. **Easy leak detection possible**
11. **Non-Toxic**
12. **Environmental friendly**
13. **Cheap**
14. **Easily available**
15. **Easily stored.**

1.7 DOUBLE EFFECT H₂O-LiBr₂ ABSORPTION SYSTEM

A single –stage like the single effect absorption system is not suited to utilize a heat source at a temperature higher than a certain point unlike other heat operated refrigerating machines that follow the Carnot trend ,viz., the higher the temperature of the heat source ,the higher the COP . In fact the COP decreases as the heat source temperature increases beyond a point. This is because the absorption system is not a reversible refrigerating machine. Because of mixing process of refrigerant and absorbent, a degree of irreversibility is involved. That is why, the COP of an absorption system levels with the increase in generator temperature , and than it starts decreasing.

It is found that the single effect system gives best results upto a heat source temperature of 105 °C. Above that temperature it is recommended to double effect system.

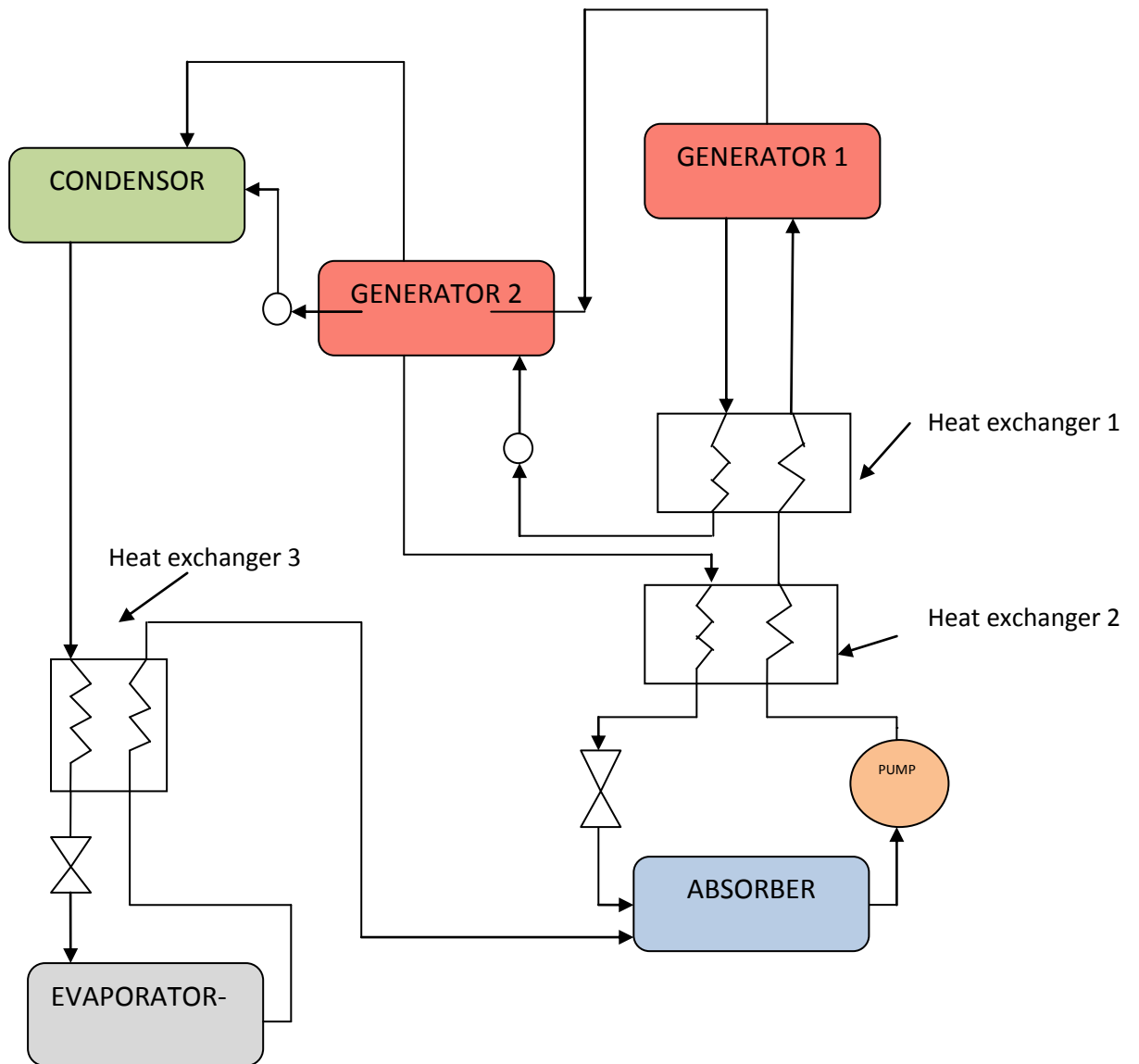


Fig. 1.4: Schematic diagram of double effect H₂O- LiBr refrigeration system

1.8 CASCADE REFRIGERATION SYSTEM

A cascade refrigeration system consists of two or more separate refrigeration systems that are connected to each other in such a way that the evaporator of the higher stage system serves a condensing medium of the lower stage system. Cascade staging incorporates several individual refrigeration systems that use different refrigerants and have closed heat exchangers to achieve low operating temperatures and reasonable condensing pressures. For some industrial applications which require moderately low temperatures, single stage vapor compression refrigeration cycles become impractical. Therefore, cascade systems are employed to obtain high temperature differentials between the heat source and heat sink. These systems are applied for temperatures ranging from -70 to 100 °C.

In low-temperature applications, including rapid freezing and the storage of frozen food, the required evaporating temperature of the refrigeration system ranges from -40 °C to -55 °C, so a single-stage vapor-compression refrigeration system is insufficient. Instead, two-stage or cascade refrigeration systems are used for low-temperature applications. The high- and low-pressure sides of a two-stage refrigeration system are charged with the same refrigerant, whereas the high and low-temperature circuits in a cascade system are filled separately with appropriate refrigerants. With respect to global environmental protection, the use of natural refrigerant in refrigeration systems has been demonstrated to be a complete solution to permanent alternative fluorocarbon-based refrigerant. Therefore, using natural refrigerants in both two-stage and cascade refrigeration system helps to satisfy the obligations of environmental treaties.

Ammonia (R717) is a natural refrigerant that is most commonly adopted in low-temperature two-stage refrigeration systems, but it has disadvantages. For instance, ammonia has a pungent smell; it is toxic and moderately flammable, and has relatively large swept volume requirements at under -35 °C. Additionally, the evaporating pressure of an ammonia system is below atmospheric pressure when the evaporating temperature is below -35 °C, causing air to leak into the refrigeration system, leading to short-term inefficiency and the long-term unreliability of the system. Hence, a nontoxic, non-flammable and dense refrigerant gas with a positive evaporating pressure should be chosen for evaporation below -35 °C. A cascade refrigeration system with natural refrigerants CO_2 and NH_3 meets these requirements.

A CO₂/NH₃ cascade refrigeration system uses ammonia and carbon dioxide as refrigerants in high- and low temperature circuits, respectively. Carbon dioxide (R744) was a commonly used natural refrigerant in vapour compression refrigeration systems for over 130 years, but it has only been fully exploited during the last decade. Some of the characteristics of CO₂ make it a good alternative to ammonia for use in large-scale refrigeration plants operated at low temperatures. The most obvious advantages of carbon dioxide are that it is nontoxic, incombustible and has no odor. Moreover, as compared with ammonia two-stage refrigeration system, the CO₂/NH₃ cascade refrigeration system has a significantly lower charge amount of ammonia, and the COP of the cascade system exceeds that of a two-stage system at low temperatures. Therefore, many investigations of the CO₂/NH₃ cascade refrigeration system are attracting attention.

In the design phase of a CO₂/NH₃ cascade refrigeration system, an important issue is the means of determining the optimal condensing temperature of a cascade-condenser under particular design conditions, such as condensing temperature, evaporating temperature and the temperature difference between the high- and low-circuits in cascade-condenser. Studies that seek to find the optimal condensing temperature of the CO₂/NH₃ cascade refrigeration system are lacking. The optimal condensing temperature of a cascade-condenser is -18 °C at a condensing temperature of 35 °C and an evaporating temperature of -50 °C. However, they reported only one specific condition and did not evaluate the effects of varying the design conditions, such as the condensing and evaporating temperatures, on the optimal condensing temperature of the cascade-condenser and its corresponding maximum COP.

1.9 COMPRESSION-ABSORPTION CASCADE REFRIGERATION SYSTEM

In the refrigeration field there are applications which require the production of very high cooling power at low temperatures, such as freezing processes and cold stores for the storage of frozen products. Currently, different configurations of vapor compression systems of double stage with ammonia or synthetic refrigerants are generally applied to this type of applications. Moreover, recently the two stage compression systems in cascade with CO₂ as refrigerant in the low temperature stage are the object of important research and nowadays there are already several industrial and commercial installations successfully running. However, the disadvantage of the compression systems in this type of applications is their high electricity consumption. The system is a two stages cascade that consists of a single stage compression system for the generation of the cooling power at low temperature and an absorption system in the high temperature stage, as shown in Fig.1.5 . Both systems share a heat exchanger, which operates simultaneously as the condenser of the compression system and as the evaporator of the absorption system. This refrigeration system would decrease the electricity consumption compared to the two stages compression systems, since it is only required to operate the compression system at the low stage; meanwhile the absorption system is driven by heat. Moreover, it could use environmentally friendly working fluids such as carbon dioxide or ammonia in the compression stage and the pairs ammonia–water or water–lithium bromide in the absorption system. this cascade refrigeration system could be integrated with a cogeneration system, since this would supply simultaneously the electricity to the compression system and the heat to the absorption system. At a first glance, it would bring an additional advantage, since the global system could be designed as a standalone device independent of the electric grid. However, making use of these benefits requires knowledge of the adaptability of the energy needs of the refrigeration system (electricity and heat) to the power distribution supplied by the cogeneration system.

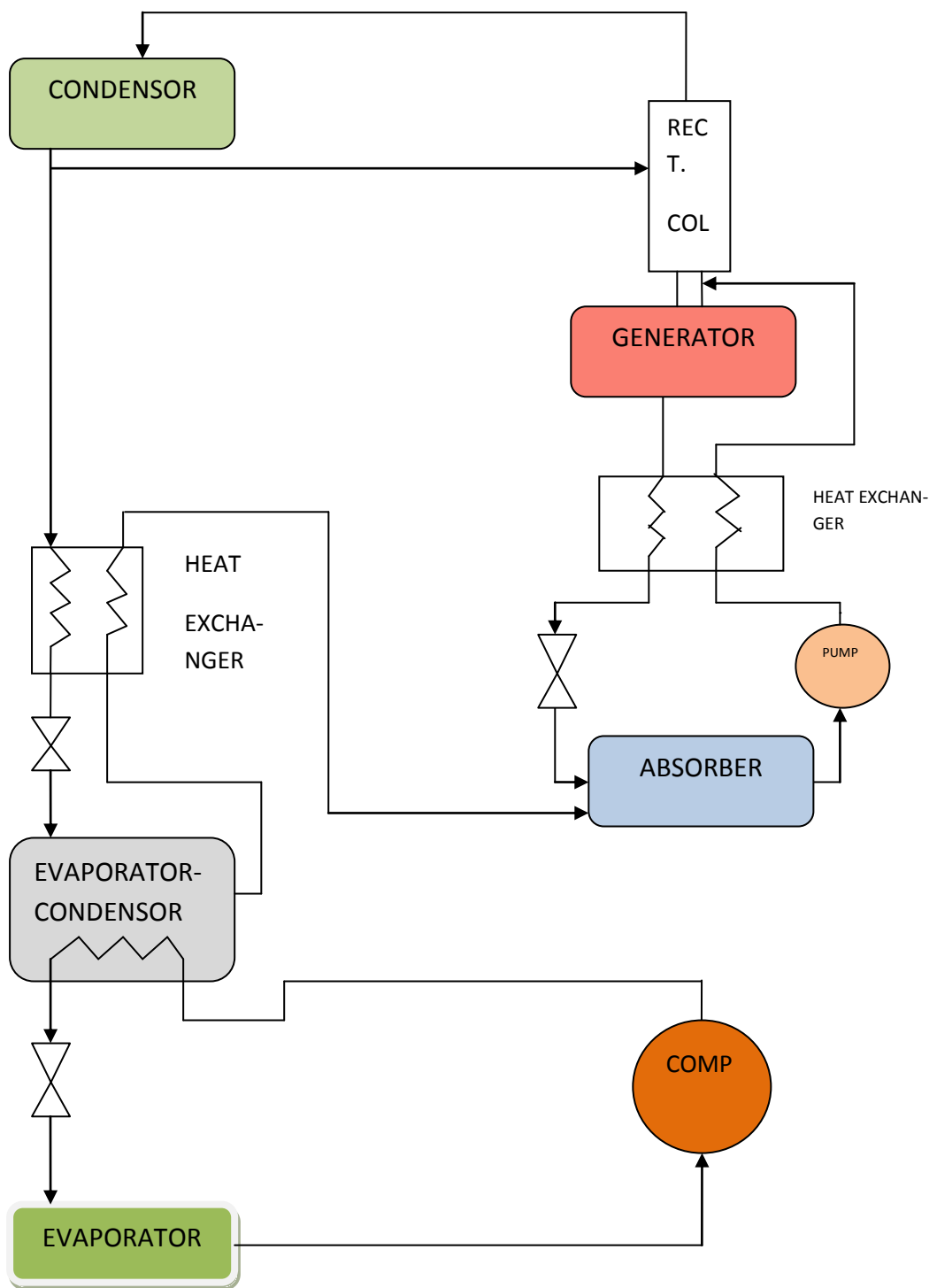


Fig.1.5 Schematic diagram of the compression-absorption cascade refrigeration system for $\text{NH}_3\text{-H}_2\text{O}$ in absorption system

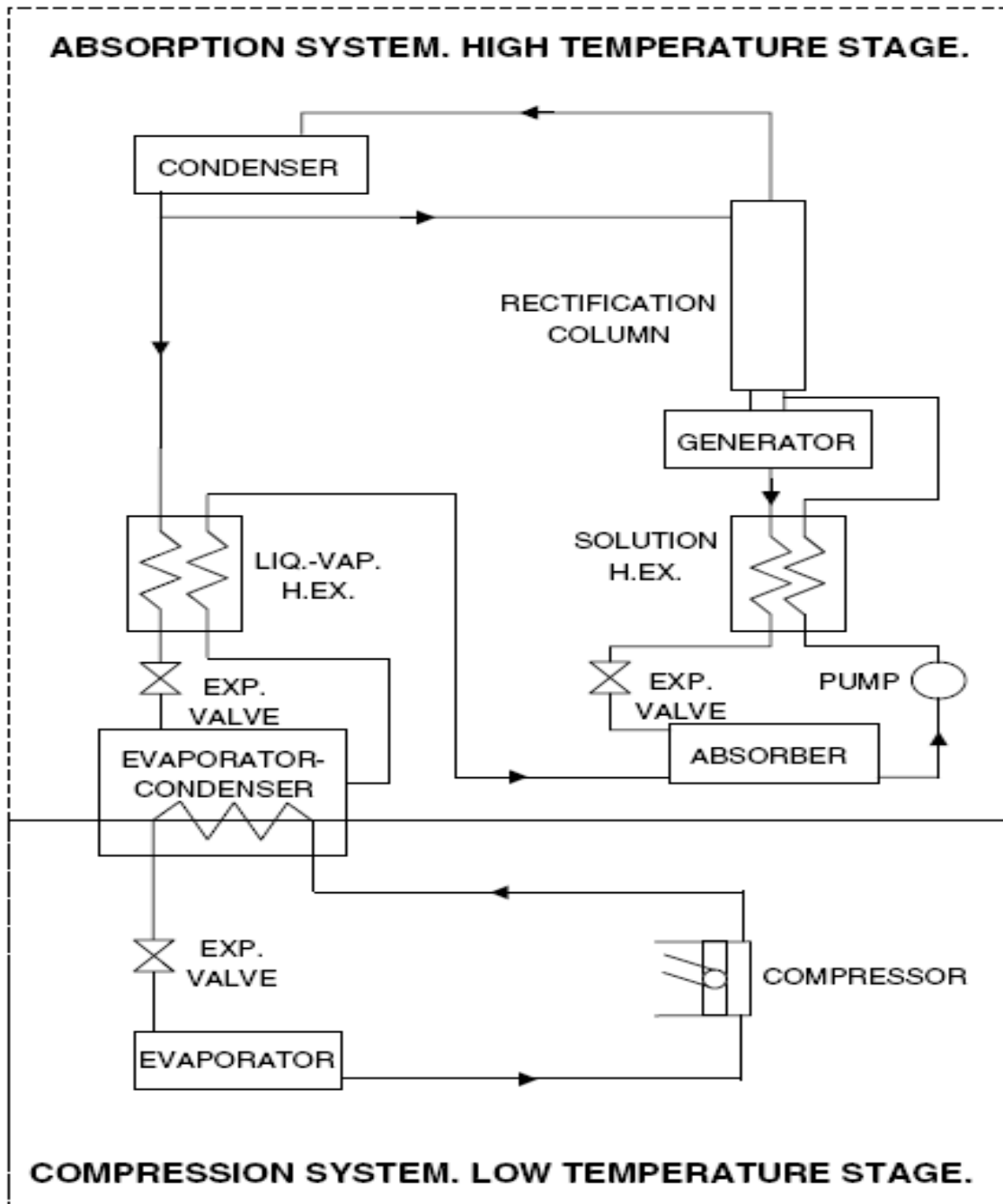


Fig1.6. Schematic diagram of the compression-absorption cascade refrigeration system

1.10 REFRIGERATION SYSTEM AND SIMULATION MODEL

The absorption–compression cascade system being considered is depicted schematically in Fig.1.7. It consists of a single stage compression system in the low temperature cascade and a single stage absorption system in the high temperature cascade. The analysis has been carried out considering natural refrigerant ammonia, in the compression system, whose main components are the evaporator, compressor, condenser and the expansion device. The absorption system uses the pair Lithium bromide–water and its major components are the absorber, generator, condenser, evaporator, solution heat exchanger, pump and two expansion devices. The compression and the absorption systems are connected to each other by means of the evaporator–condenser heat exchanger.

A simple steady state simulation model based on sequential modular approach has been developed and implemented in a computer program. The model equations are formulated from species, mass and energy balances. In the model, the components irreversibilities are defined either directly by means of temperature differences or by means of the components efficiency.

Efficiency of the evaporator– condenser heat exchanger is assumed; hence the cooling duty of the absorption system is equated to the condensation power of the compression system by using efficiency of evaporator condenser heat exchanger. The condensation temperature of the compression system together with the temperature difference between this temperature and the evaporation temperature at the absorption system are used to characterise the heat transfer processes in the evaporator–condenser heat exchanger. The condensation temperature at the compression system is taken as design parameter to define the intermediate temperature level. In the absorption system, the following assumptions are taken into account; the refrigerant solution leaving the condenser and the weak solution leaving the generator are saturated at condensation and generation temperature, respectively.

The objective is to simulate and analyse the influence of the key design parameters and the operating conditions on the performance of the compression–absorption cascade refrigeration system.

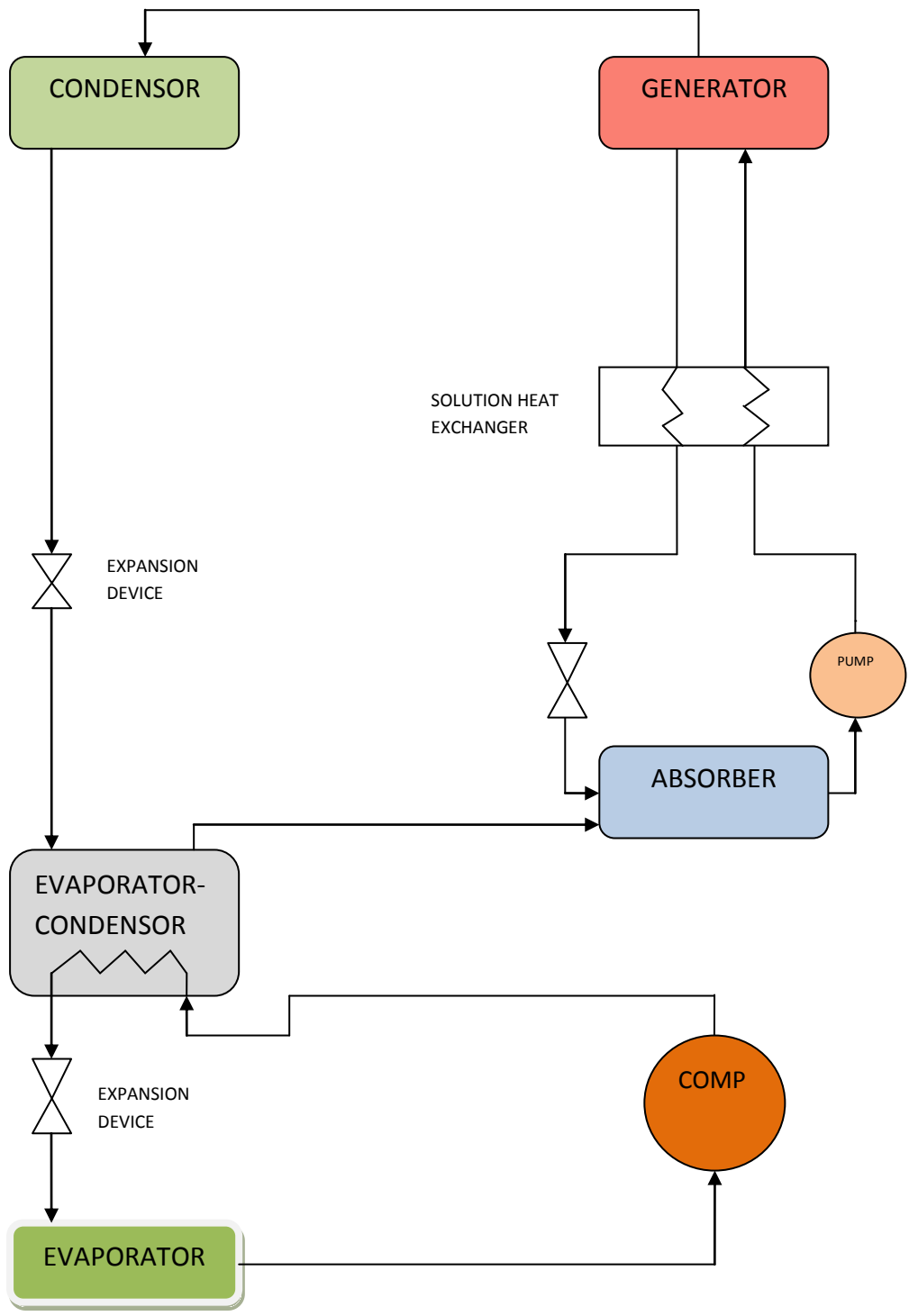


Fig. 1.7: Schematic diagram of the compression-absorption cascade refrigeration system for Li-Br –H₂O in absorption and NH₃ in compression system

2.1 Summary

The thermodynamic processes in the absorption refrigeration system release a large amount of heat to the environment. This heat is evolved at temperatures considerably above the ambient temperature, which results in a major irreversible loss in the system components. According to M.M. Talbi and B. Agnew [1] an exergy analysis is carried out on a single-effect absorption refrigeration cycle with lithium-bromide + water as the working fluid pair. Numerical results for the cycle are tabulated. A design procedure has been applied to a lithium-bromide absorption cycle and an optimisation procedure that consists of determining the enthalpy, entropy, temperature, mass flow rate, heat rate in each component, and coefficient of performance has been performed. A computer program has been developed to predict the performance of an absorption refrigeration unit. A basic thermodynamic analysis of the LiBr absorption-refrigeration cycle has been performed and the dimensionless total exergy loss and exergy loss of each component are calculated. Consequently, the results of the second law analysis can be used to identify the less efficient components of the system. The load in the condenser is slightly higher than that in the evaporator due to primarily superheating of the inlet vapour to the condenser. The condenser and evaporator loads are approximately 27.8% less than the corresponding generator and absorber loads. This difference is largely due to the heat of mixing in the solution, which are not present in the pure fluids. It has been shown that the absorption refrigeration cycle is effective in demonstrating the advantages of the exergy method since there are large irreversible losses in the heat transfer process that are not accounted for in the conventional heat balance.

According to R.D. Misra et al.[2], the thermoeconomic theory is applied to the economic optimization of a single effect water/LiBr vapour absorption refrigeration system for air-conditioning application, aimed at minimizing its overall operation and amortization cost. The mathematical and numerical techniques based optimization of thermal system is not always possible due to plant complexities. Therefore, a simplified cost minimization

methodology is applied to evaluate the economic costs of all the internal flows and products of the system by formulating exergoeconomic cost equations. Once these costs are determined, the system is thermoeconomically evaluated to identify the effects of design variables on costs and enables to suggest values of design variables that would make the overall system cost effective. Finally, an approximate optimum design configuration is obtained by means of sequential local optimization of the system, carried out unit by unit. The result compares this optimum with the base case and shows percentage variations in the system's operation and amortization cost.

R.D. Misra et al. [3] the thermoeconomic concept is applied to the optimization of a double-effect H₂O/LiBr VAR system, aimed at minimizing its overall product cost. A simplified cost minimization methodology based on the thermoeconomic concept is applied to calculate the economic costs of all the internal flows and products of the system by formulating thermoeconomic cost balances. Once these costs are determined, the system is thermoeconomically evaluated to identify the effects of the design variables on cost of the flows and products. This enables to suggest changes of the design variables that would make the overall system cost-effective. Finally, an approximate optimum design configuration is obtained by means of an iterative procedure. The result shows significant improvement in the system performance. The sensitivity analysis shows that the changes in optimal values of the decision variables are negligible with changes in the fuel cost. It demonstrates the application of the thermoeconomic evaluation and optimization method to optimize a double-effect H₂O/LiBr VAR system. Moreover, it is observed that the thermoeconomic analysis of a system is able to provide suggestions about potential cost-effective improvements achievable by means of changes in the values of the internal operating parameters (decision variables in the present case) of the system.

Jose Fernandez-Seara et al. [4] describes the study carried out to analyse a refrigeration system in cascade with a compression system at the low temperature stage and an absorption system at the high temperature stage to generate cooling at low temperatures, as well as the possibility of powering it by means of a cogeneration system. CO₂ and NH₃ have been considered as refrigerants in the compression stage and the pair NH₃-H₂O in the absorption stage. The analysis has been realized by means of a mathematical model of the refrigeration system implemented in a computer program and taking into account the characteristic operating conditions of a cogeneration system with gas engines. Jose Fernandez-Seara et al. presents the results obtained regarding the performance of the refrigeration system and the

adaptability between the power requirements of the refrigeration system and the power supplied by the cogeneration system.

Berhane H. Gebreslassie et al. [5] The performance of seven different water–LiBr absorption cooling cycles has been evaluated applying first and second law analysis. Only unavoidable exergy destruction is considered in order to compare the cycles on a rational basis. Effects of the avoidable exergy destructions are eliminated at this stage of the theoretical analysis, but should be considered at the design stage. The avoidable part shows where the main potential for improvement of the cycle is. This is not necessarily the component with the largest exergy destruction, if the exergy destruction is mainly due to the unavoidable part. The effect of the heat source temperature has been evaluated for typical cooling operating conditions. The COP increases from half to triple effect and shows for each cycle a maximum, which is slightly higher than the cut-off temperature. The values of the COP are higher than in studies which include both avoidable and unavoidable exergy destruction and maintain these high values also close to the cut-off temperature. At higher heat source temperatures the COP decreases slowly. The same qualitative behavior is found for the exergetic efficiency. But the decrease at higher heat source temperatures is more significant as in the denominator of the exergetic efficiency the heat rate to the generator is nearly constant, while its temperature and thus the dimensionless exergetic temperature is increasing. As a consequence the exergy input (Fuel) increases, while the output (Product) in the numerator is fixed. The maximum exergy efficiencies are lowest for the half effect, followed by the single effect. Highest values are found for double and triple effect. Little difference is found among the flow configurations (reverse, series and parallel flow).

R.D. Misra et al. [6] presents the thermoeconomic concept that is applied to the optimization of an aqua-ammonia vapour-absorption refrigeration (VAR) system—aimed at minimizing its overall product cost. The thermoeconomic concept based simplified cost minimization methodology calculates the economic costs of all the internal flows and products of the system by formulating thermoeconomic cost balances. The system is then thermoeconomically evaluated to identify the effects of design variables on costs and thereby enables to suggest values of design variables that would make the overall system cost-effective. Based on these suggestions, the optimization of the system is carried out through an iterative procedure. The results show a significant improvement in the system performance without any additional investment. Finally, sensitivity analysis is carried out to study the effect of the changes in fuel cost to the system parameters.

B. Kundu et al. [7] effort has been devoted to analyze the collector performance parameters of a solar-assisted LiBr/H₂O vapor absorption cooling system with a flat-plate collector consisting of an absorber plate of different profiles. The effect of the collector fluid inlet temperature on the performance of solar collector, vapour absorption cycle, vapor absorption system and refrigerating efficiency has been studied for a wide range of design variables. A comparative study has also been made among the performance parameters of an absorber plate of different shapes with the variation of collector fluid inlet temperature. From the result, it can be highlighted that, at a particular collector fluid inlet temperature, the performances of a vapor absorption system attain a maximum value. Finally, an optimum collector fluid inlet temperature is determined by satisfying the minimization of volume of an absorber plate without affecting the cooling rate in the evaporator.

Yuyuan Wu et al. [8] improved system of NH₃-H₂O-LiBr was proposed for overcoming the drawback of NH₃-H₂O absorption refrigeration system. The LiBr was added to NH₃-H₂O system anticipating a decrease in the content of water in the NH₃-H₂O -LiBr system. An equilibrium cell was used to measure thermal property of the ternary NH₃-H₂O -LiBr mixtures. The pressure-temperature data for their vapor-liquid equilibrium (VLE) data were measured at ten temperature points between 15-85 °C, and pressures up to 2 MPa. The LiBr concentration of the solution was chosen in the range of 5-60% of mass ratio of LiBr in pure water. The VLE for the NH₃-H₂O -LiBr ternary solution was measured statically. The experimental results show that the equilibrium pressures reduced by 30-50%, and the amount of component of water in the gas phase reduced greatly to 2.5% at T=70 °C. The experimental results predicted much better characteristics of the new ternary system than the NH₃-H₂O system for the applications.

A. Kilicarslan [9] experimental investigated and theoretical studied of a different type of two-stage vapor compression cascade refrigeration system using R-134 as the refrigerant are presented. Performance evaluations of two single stage vapor compression systems and two-stage vapor compression refrigeration cascade system are performed with respect to theoretical model developed. In the first section of the experiments, one refrigeration system, namely RU2, is operated. During the experiments, rate of the water flow connecting both systems is kept constant at various values and the voltage across evaporator heaters is increased from 100 to 200 V with intervals of 20 V. In the second part of the first category, experiments are repeated by using different mass flow rates of water. In the second section, two separate refrigeration systems, namely RU1 and RU2 are connected to each other by

using the water loop. This system is also called cascade refrigeration system. It is observed that the change in water mass flow rate has little effect on the coefficient of performance for single stage and cascade stage refrigeration systems. It is also observed that the coefficient of performance is mainly a function of evaporator temperature and pressure. When RU2 operating in the single stage refrigeration system is compared with RU2 operating in the two-stage cascade refrigeration system at the same refrigeration load interval (360–460 W), the average percentage values of the decrease in the condensing pressure, the decrease in the compressor power and the increase in the COP are 21.9, 31.7 and 32.7, respectively.

According to Paul Kalinowski et al. [10] the recovery process of the liquefied natural gas requires low temperature cooling, which is typically provided by the vapor compression refrigeration systems. The usage of an absorption refrigeration system powered by waste heat from the electric power generating gas turbine could provide the necessary cooling at reduced overall energy consumption. A potential replacement of propane chillers with absorption refrigeration systems was theoretically analyzed. From the analysis, it was found that recovering waste heat from a 9 megawatts (MW) electricity generation process could provide 5.2 MW waste heat produced additional cooling to the LNG plant and save 1.9 MW of electricity consumption. Application of the integrated cooling, heating, and power is an excellent energy saving option for the oil and gas industry.

Jaime Sieres et al. [11] presents an analysis of the influence of the distillation column components size on the vapour enrichment and system performance in small power $\text{NH}_3\text{--H}_2\text{O}$ absorption machines with partial condensation. It is known that ammonia enrichment is required in this type of systems; otherwise water accumulates in the evaporator and strongly deteriorates the system performance and efficiency. The distillation column analysed consists of a stripping adiabatic section below the column feed point and an adiabatic rectifying packed section over it. The partial condensation of the vapour is produced at the top of the column by means of a heat integrated rectifier with the strong solution as coolant and a water cooled rectifier. Differential mathematical models based on mass and energy balances and heat and mass transfer equations have been developed for each one of the column sections and rectifiers, which allow defining their real dimensions. Results are shown for a given practical application. Specific geometric dimensions of the column components are considered. Different distillation column configurations are analysed by selecting and discarding the use of the possible components of the column and by changing their

dimensions. The analysis and comparison of the different column arrangements has been based on the system COP and on the column dimensions.

I. Horuza and T.M.S. Callander [12] described experimental investigation of the performance of a commercially available vapor absorption refrigeration (VAR) system. The natural gas-fired VAR system uses aqua-ammonia solution with ammonia as the refrigerant and water as the absorbent and has a rated cooling capacity of 10 kW. The unit was extensively modified to allow fluid pressures and temperatures to be measured at strategic points in the system. The mass flow rates of refrigerant, weak solution, and strong solution were also measured. The system as supplied incorporates air-cooled condenser and absorber units. Water-cooled absorber and condenser units were fitted to extend the VAR unit's range of operating conditions by varying the cooling water inlet temperature and/or flow rates to these units. The response of the refrigeration system to variations in chilled water inlet temperature, chilled water level in the evaporator drum, chilled water flow rate, and variable heat input are presented.

An experimental investigation by S. Arivazhagan et al. [13] on the performance of a two-stage half effect vapour absorption cooling system has been carried out and presented. The prototype is designed for 1 kW cooling capacity using HFC based working fluids (R134a as refrigerant and DMAC as absorbent). The performance of the system in terms of degassing range, coefficient of performance and second law efficiency has been obtained. The system is capable of producing evaporating temperature as low as -7°C with generator temperatures ranging from 55 to 75°C . The degassing range is 40% more in high absorber than in low absorber as the high absorber is operated at optimum intermediate pressure. The optimum generator temperature is found to be in the range of 65 – 70°C at which the coefficient of performance is 0.36.

During the past decade, there has been unprecedented research interest in vapour-absorption cycle refrigeration and heat pumping driven by the need to reduce CO_2 emissions related to process and comfort cooling. Shenyi Wu and Ian W. Eames [14] reviews some recent innovations in vapour absorption-cycle technology, with particular emphasis on the cycle design and fluid selection. The operation and design of innovative cycles are described as well as the latest research in working fluids.

Simulation has been widely used for performance prediction and optimum design of refrigeration systems. A brief review on history of simulation for vapour-compression

refrigeration systems is done. Guo-liang Ding [15] summarized models for evaporator, condenser, compressor, capillary tube and envelop structure. Some developing simulation techniques, including implicit regression and explicit calculation method for refrigerant thermodynamic properties, model-based intelligent simulation methodology and graph-theory based simulation method, are presented. Prospective methods for future simulation of refrigeration systems, such as noise-field simulation, simulation with knowledge engineering methodology and calculation methods for nanofluid properties, are introduced briefly.

The construction of a triple-effect absorption cooling machine using the lithium bromide-based working fluid is strongly limited by the corrosion problem caused by the high generator temperature. Jin-Soo Kim et al. [16] suggested four compressor-assisted H₂O/LiBr cooling cycles to solve the problem by lowering the generator temperature of the basic theoretical triple-effect cycle. Each cycle includes one compressor at a different state point to elevate the pressure of the refrigerant vapor up to a useful condensation temperature. Cycle simulations were carried out to investigate both a basic triple-effect cycle and four compressor assisted cycles. All types of compressor-assisted cycles were found to be operable with a significantly lowered generator temperature. The temperature decrements increase with elevated compression ratios. This means that, if a part of energy input is changed from heat to mechanical energy, the machine can be operated in a favorable region of generator temperature not to cause corrosion problems. In order to obtain 40 K of generator temperature decrement (from 475.95 K) for all cycles, 3–5% of cooling capacity equivalent mechanical energies were required for operating the compressor. A great advantage of the investigated triple-effect cycles is that the conventionally used H₂O/LiBr solution can be used as a working fluid without the danger of corrosion or without integrating multiple solution circuits.

A simulation analysis was carried out for three kinds of triple-effect absorption cycles of parallel-flow, series-flow and reverse-flow using a newly developed simulation program. Y. Kaita [17] investigated the cycles are similar to the alternate double-condenser coupled cycles of Grossman. The coefficient of performance, the maximum pressure and the maximum temperature of each cycle were calculated. The sensitivity analysis of UA of each component was also carried out. The results show that the parallel-flow cycle yields the highest coefficient of performance among the cycles, while the maximum pressure and temperature in the reverse-flow cycle are lower than those of other cycles.

Tzong-Shing Lee's [18] study thermodynamically analyzed a cascade refrigeration system that uses carbon dioxide and ammonia as refrigerants, to determine the optimal condensing temperature of the cascade-condenser given various design parameters, to maximize the COP and minimize the exergy destruction of the system. The design parameters include: the evaporating temperature, the condensing temperature and the temperature difference in the cascade-condenser. The results agreed closely with the reported experimental data. The optimal condensing temperature of the cascade-condenser increases with TC, TE and DT. The maximum COP increases with TE, but decreases as TC or DT increases. Two useful correlations that yield the optimal condensing temperature of the cascade-condenser and the corresponding maximum COP are presented.

A cascade refrigeration system with CO₂ and NH₃ as working fluids in the low and high temperature stages, respectively, has been analysed by J. Alberto Dopazo et al. [19]. Results of COP and exergetic efficiency versus operating and design parameters have been obtained. In addition, an optimization study based on the optimum CO₂ condensing temperature has been done. Results show that following both method's exergy analysis and energy optimization, an optimum value of condensing CO₂ temperature is obtained. The compressor isentropic efficiency influence on the optimum system COP has been demonstrated. A methodology to obtain relevant diagrams and correlations to serve as a guideline for design and optimization of this type of systems has been developed and it is presented in the paper.

MATHEMATICAL MODELLING OF COMPRESSION- ABSORPTION CASCADE REFRIGERATION SYSTEM

3.1 SYSTEM DESCRIPTION

A schematic diagram of the cascade system is shown in figure3.1. The cascade refrigeration system is constituted by two single stage systems connected by a heat exchanger (cascade heat exchanger). The low temperature system with NH_3 as refrigerant is used for cooling. The high temperature system (LiBr- H_2O Vapour absorption system) water as refrigerant is used to condensate the NH_3 of the low temperature system.

In the evaporator, the NH_3 at the evaporating temperature absorbs the cooling duty Q_{evap} (NH_3) from the cooling space (at T_{21} °C temperature), then is compressed in the NH_3 compressor and condensed in the cascade heat exchanger at a condensing temperature of T_{con} NH_3 , and then sent to the expansion valve from which the evaporator is supplied. In the condenser, the heat flo Q_{con} is removed from the Water at condensing temperature of T_c H_2O to condensing medium (at T_0 temperature). The H_2O is expanded, then evaporated at an evaporating temperature of T_e H_2O in the cascade heat exchanger, and then absorbed in the absorber and pumped into the generator.

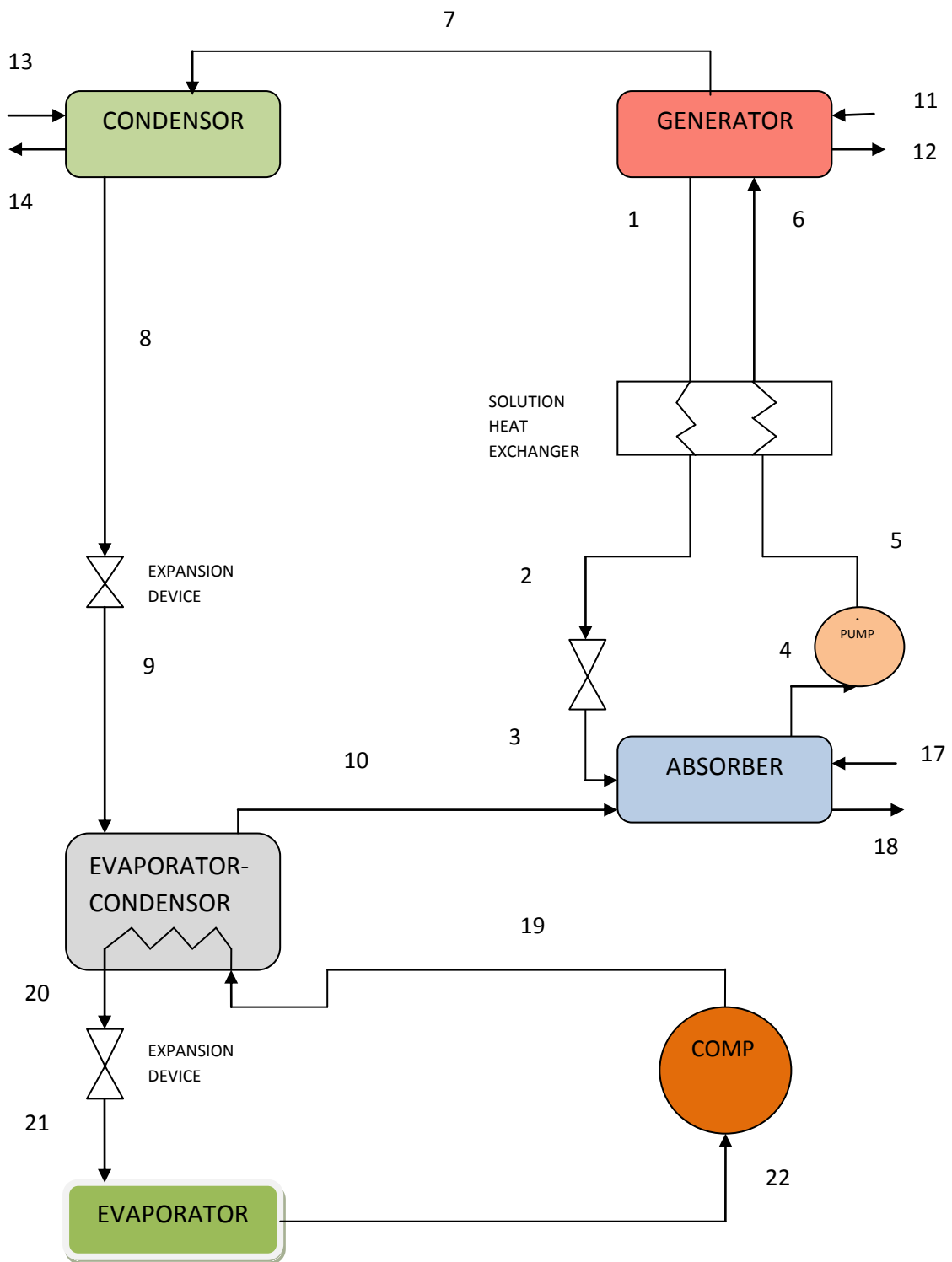


Fig.3.1 Schematic diagram of the compression-absorption cascade refrigeration system for Li-Br-H₂O in absorption system and NH₃ in compression system

3.2 MODELLING APPROACH

The thermodynamic processes in the absorption refrigeration system release a large amount of heat to the environment. This heat is evolved at temperatures considerably above the ambient temperature, which results in a major irreversible loss in the system components. A design procedure has been applied to a lithium-bromide absorption cycle and vapour compression cycle that consists of determining the enthalpy, entropy, temperature, mass flow rate, heat rate in each component, and coefficient of performance has been performed.

Energy and exergy methods are well-established methods, which are used to study energy conversion processes. The exergy method, known as the second law analysis, calculates the exergy loss caused by irreversibility, which is an important thermodynamic property which measures the useful work that can be produced by a substance or the amount of work needed to complete a process. Unlike energy, exergy is not conserved; analysis of exergy losses provides information as to where the real inefficiencies in a system lie. The equations of mass, energy and exergy balance for absorption cycle are taken from literature [1].

3.2.1 ASSUMPTIONS

1. Heat losses through the system components are negligible.
2. Solution leaving the absorber and the generator are assumed to be saturated in equilibrium conditions at their respective temperatures and concentrations.
3. Refrigerants at the cascade heat exchanger outlets, condenser outlet and evaporator outlet, are saturated.
4. Refrigerant vapour leaving the generator is considered to be superheated.
5. The reference enthalpy (h_o) and entropy (s_o) used for calculation of the working fluid are the values for water at an environmental temperature and pressure of 35 °C and 1 bar respectively.
6. Pressure losses in connecting pipes and heat exchangers have been neglected

3.2.2 Exergy Method

A second law analysis calculates the system performance based on exergy, which always decreases, owing to thermodynamic irreversibility. Exergy analysis is the combination of the first and second law of thermodynamics and is defined as the maximum amount of work potential of a material or a form of energy in relation to the surrounding environment. Therefore, in an exergy analysis the losses represent the real losses of work. The principle irreversibilities in a process leading to these losses are due to

- Dissipation (friction).
- Heat transfer under temperature difference.
- Unrestricted expansion.

The exergy content of a pure substance is generally given by

$$\Psi = (h - h_0) - T_0(s - s_0) \quad \dots\dots\dots(1)$$

where the terms h_0 and s_0 are the enthalpy and entropy values of the fluid at the environmental temperature T_0 , which ultimately forms the energy (heat) sink for all irreversible and reversible processes. However, in a binary mixture solution such as LiBr and water, the concentration of the mixture must be taken into account for exergy calculation. For a dead state defined as the environmental state at T_0 , the exergy of the solution is calculated by

$$\Psi = [h(T, X) - h_0] - T_0 [s(T, X) - s_0] \quad \dots\dots\dots(2)$$

The availability loss in each component is calculated by:

$$\Delta \Psi = \sum m_i \Psi_i - \sum m_E \Psi_E - Q(1 - T_0/T) - W \quad \dots\dots\dots(3)$$

The first term on the right-hand side is the sum of the exergy input. The second is the sum of the exergy output, while the third term is the exergy of heat Q , which is transferred at constant temperature T . The exergy of heat is equal to the work obtained by a Carnot engine operating between T and T_0 and is therefore equal to the maximum reversible work that can be obtained from heat energy Q . The last term is the mechanical work transfer to or from the system. The total energy of the absorption refrigeration cycle is the sum of the exergy loss in each component, therefore:

$$\Delta \psi_T = \Delta \psi_G + \Delta \psi_C + \Delta \psi_{v1} + \Delta \psi_E + \Delta \psi_A + \Delta \psi_{v2} + \Delta \psi_{she} + \Delta \psi_p \dots(4)$$

3.2.3 Modelling of each component

Energy and mass balances were written around each of the components and combined with the state equations for the thermodynamic properties of the lithium-bromide and water to yield a set of equations describing the system. The state equations were evaluated by the thermodynamic properties of LiBr and water. The principles of the optimisation lies in the identification and minimisation of the sources of lost work within the refrigeration cycle. The operating characteristics of the system components including the heat exchangers and the temperature differences between the internal fluids and those between the external fluids are factors considered in the analysis. In this case, the heat transfer values were reproduced by involving the energy balances on each of the components. Therefore, in order to determine the heat and mass transfer as well as the thermodynamic properties of the components, each component is taken as a single unit, the balance equations of mass, energy, entropy, heat transfer and exergy balance can be found in more details in the analysis.

3.3 VAPOUR ABSORPTION CYCLE ANALYSIS

The absorption refrigeration cycle has been analysed thermodynamically as illustrated in Fig3.2. in a schematic form. The generator heats using waste gas at 500 °C, and an ambient of 35 °C was used as a cooling medium for the absorber, condenser and evaporator. The model considered consisted of an internal and an external system. The external system represented the connection between the internal system and the surroundings. The internal system was a standard absorption cycle containing evaporator, condenser, absorber, generator, pump, two- expansion valves and solution heat exchanger. The external system was given by three open-air circuits and one as a heat source to the cycle carrying heat from or to the internal system. A schematic diagram of the system energy balance for absorption cycle is shown in Fig. 3.2 and the equivalent availability flow balance is shown in Fig. 3.3.

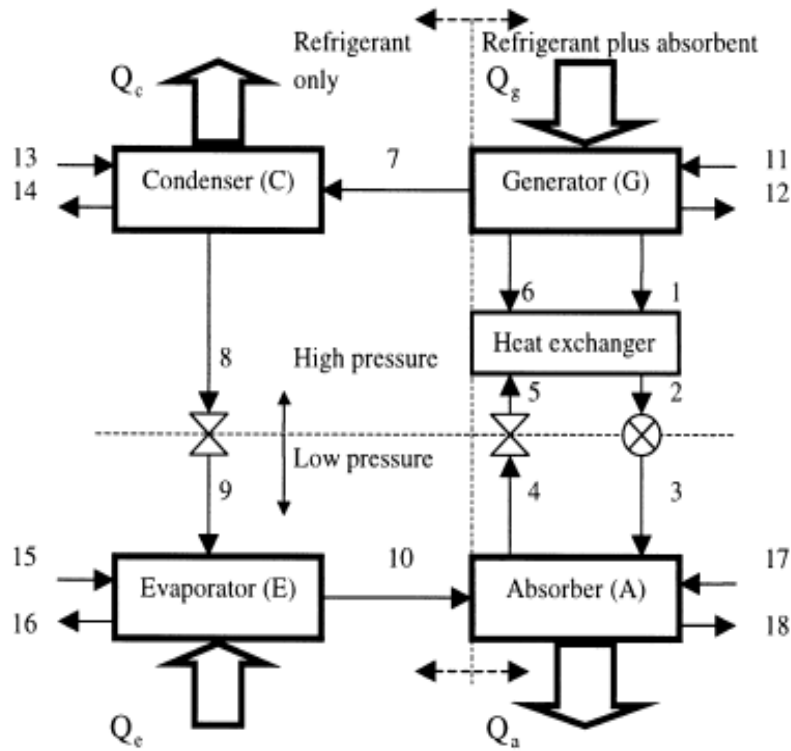


Fig.3.2. Energy Flow balance for absorption cycle.

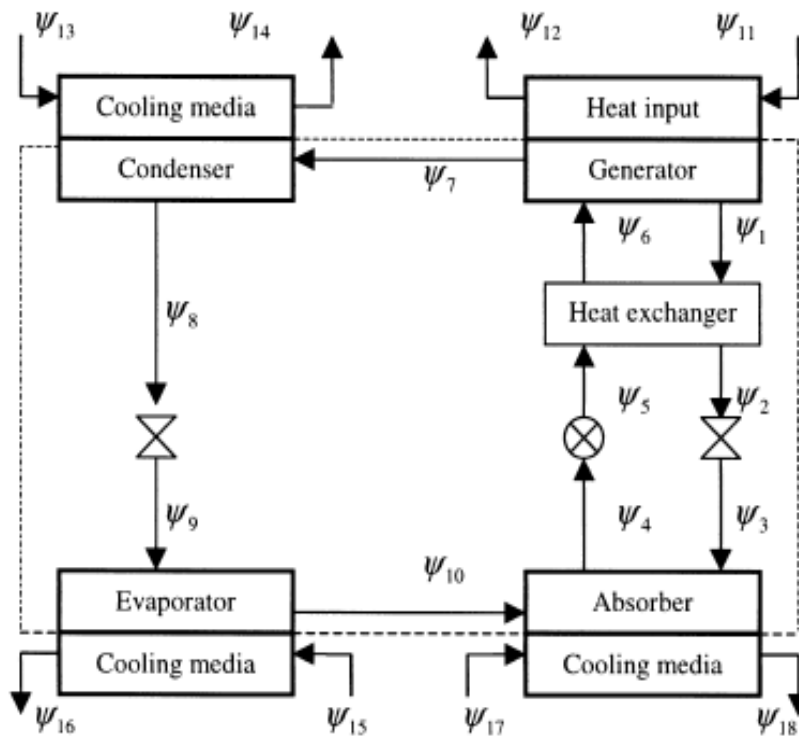


Fig. 3.3. Availability flow balance for the absorption cycle.

The computer program was based on heat and mass balances, heat transfer equations, and thermodynamic property reactions written in terms of the static point properties for each of the subunits and matched at the connecting points. The initial conditions read into the program included the ambient conditions, component temperature, mass fraction, and effectiveness, vapour and cold airflow rates. With the given parameters, the program calculated the thermodynamic properties of the mixture at all points in the cycle. The COP was also calculated, which is defined as the ratio of the generator load to the evaporator load. The computer program was written in EES.

3.3.1 Enthalpy and entropy calculation

In the condenser

$$h_1 = -1295.60965501 + 560.49216796T - 43.7942784871T^2 + 4.479367474097T^3 + 1.268510765098P - 2.34584584613 \times 10^{-4}P - 3.87145821 \times 10^{-2}PT^2 \text{ (KJ/kg)} \dots\dots\dots(A1)$$

Similarly, the specific entropy of the liquid water,

$$s_1 = -3.7415015475 + 5.604921679618 \log T - 0.8758855697420T + 6.71905121 \times 10^{-2}T^2 + 2.054551464 \times 10^{-3}P - 7.7429164 \times 10^{-4} \times PT + 3.09716657 \times 10^{-5}T \text{ (KJ/kg K)} \dots\dots\dots(A2)$$

Meanwhile, in the evaporator and the vapour generator,

$$h_v = 1997.854583553 + 0.9857789261768P + 185.4761288854T - 1.194203005662T^2 + 0.3002594147055T^3 - 5850.240980017 P/T^3 - 25665290.31128P/T^{11} \text{ (kJ/kg)} \dots\dots\dots(A3)$$

Similarly,

$$S_v = 3.910172967373 + 1.85476128854 \log T - 2.38840601 \times 10^{-2} T + 4.50389122 \times 10^{-3} T^2 - 0.46147868561 \log P - 43.87680735012 \times P/T^4 - 235265.1611867 P/T^{12} \text{ (kJ/kg K) } \dots\dots\dots(A4)$$

Where, in Eqs. (A1)-(A4), the P is in bar/10 and the temperature T is in K/100. The specific enthalpy of the H2O/LiBr solution in the case of generator, solution heat exchanger, and absorber can be calculated in terms of the solution temperature T and mass fraction x by;

$$h = E_1(x) + E_2(x) T + E_3(x) T^2 \text{ (kJ/kg)} \dots\dots\dots(A5)$$

where,

$$E_1(x) = -2024.18588321 + 163.2976010204x - 4.881268653177x^2 + 6.30250843 \times 10^{-2} x^3 - 2.91350364 \times 10^{-4} x^4 \dots\dots\dots(A6)$$

$$E_2(x) = 18.2816227619 - 1.169094163968x - 3.24785672 \times 10^{-2} x^2 - 4.03390218 \times 10^{-4} x^3 - 1.85192774 \times 10^{-6} x^4 \dots\dots\dots(A7)$$

$$E_3(x) = -3.70056321 \times 10^{-2} + 2.88756514 \times 10^{-3} x - 8.13075689 \times 10^{-5} x^2 + 9.91097142 \times 10^{-7} x^3 - 4.44381071 \times 10^{-9} x^4 \dots\dots\dots(A8)$$

where, the temperature T is in C and x is in %.

A computer program has been written for the entropy values, which are read from the table at the same temperature and mass fraction.

3.3.2. Energy analysis

$$Q_G = m_7 h_7 + m_1 h_1 - m_6 h_6 = m_{12} (h_{12} - h_{11}) \dots\dots\dots(B1)$$

$$Q_C = m_w (h_7 - h_1) = m_{14} (h_{14} - h_{13}) \dots\dots\dots(B2)$$

$$Q_E = m_w (h_{10} - h_9) = m_w (h_{10} - h_8) \dots\dots\dots(B3)$$

$$Q_A = m_s h_3 + m_{10} h_{10} - m_4 h_4 = m_{ss} h_2 + m_w h_{10} - m_{ws} h_4 \dots\dots\dots(B4)$$

$$Q_{she} = m_{ss} (h_1 - h_2) = m_{ws} (h_6 - h_5) \dots\dots\dots(B5)$$

Mass flow analysis, Fig.3.4:

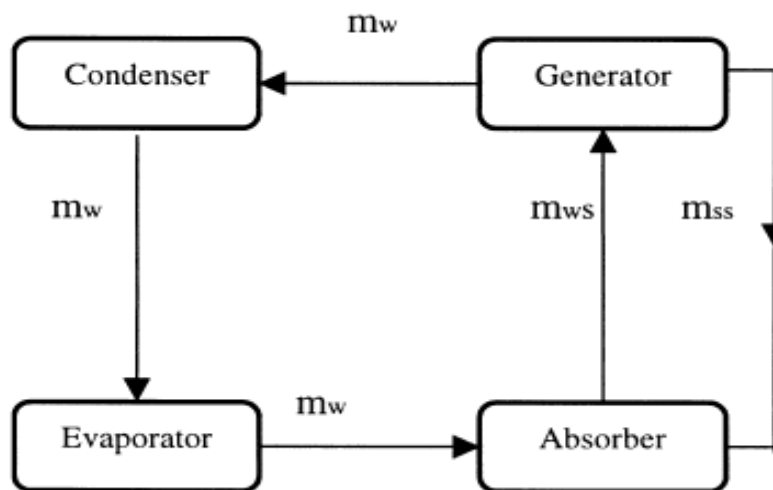


Fig.3.4 Mass balance of the cycle

$$m_{ws} = m_w + m_{ss} \dots\dots\dots(B6)$$

or; $m_6 = m_7 + m_1 \dots\dots\dots(B7)$

$$m_{ws} = m_1 = m_w \left| \frac{x_{ss}}{x_{ws} - x_{ss}} \right| = m_1 \left| \frac{x_6}{x_1 - x_6} \right| \dots\dots\dots(B8)$$

$$m_{ss} = m_6 = m_w \left| \frac{x_{ws}}{x_{ws} - x_{ss}} \right| = \left| \frac{x_1}{x_1 - x_6} \right| \dots\dots\dots(B9)$$

$$COP = \frac{Q_E}{Q_G} = \frac{m_w (h_{10} - h_8)}{m_w h_7 + m_{ss} h_1 - m_{ws} h_6} \dots\dots\dots(B10)$$

3.3.3. Exergy analysis

Generator:

$$\Delta\psi_{G,ht} = Q_G \left| 1 - \frac{T_0}{T_G} \right| - m_{12}(\psi_{12} - \psi_{11}) \dots\dots\dots(C1)$$

$$\Delta\psi_{G,in} = m_7\psi_7 + m_1\psi_1 - m_6\psi_6 - Q_G \left| 1 - \frac{T_0}{T_G} \right| \dots\dots\dots(C2)$$

$$\Delta\psi_{g,hi} = m_{12} (\psi_{12} - \psi_{11}) \dots\dots\dots(C3)$$

Condenser

$$\Delta\psi_{cm} = m_{13} (\psi_{14} - \psi_{13}) \dots\dots\dots(C4)$$

$$\Delta\psi_{c,ht} = Q_c \left| 1 - \frac{T_0}{T_C} \right| - m_{13} (\psi_{14} - \psi_{13}) \dots\dots\dots(C5)$$

$$\Delta\psi_{c,in} = m_7 (\psi_7 - \psi_8) - Q_c \left| 1 - \frac{T_0}{T_C} \right| \dots\dots\dots(C6)$$

Refrigerant expansion valve:

$$\Delta\psi_{v1} = \psi_8 - \psi_9 \dots\dots\dots(C7)$$

Evaporator:

$$\Delta\psi_{E,ht} = Q_E \left| 1 - \frac{T_0}{T_E} \right| - m_{16} (\psi_{15} - \psi_{16}) \dots\dots\dots(C8)$$

$$\Delta\psi_{E,in} = m_{10} (\psi_{10} - \psi_9) - Q_E \left| 1 - \frac{T_0}{T_E} \right| \dots\dots\dots(C9)$$

$$\Delta\psi_{cm} = m_{16} (\psi_{15} - \psi_{16}) \dots\dots\dots(C10)$$

Solution expansion valve:

$$\Delta\psi_{sol-valve} = \psi_3 - \psi_2 \dots\dots\dots(C11)$$

Absorber:

$$\Delta\psi_{A,ht} = Q_A \left| 1 - \frac{T_0}{T_A} \right| - m_{17} (\psi_{18} - \psi_{17}) \dots\dots\dots(C12)$$

$$\Delta\psi_{A,in} = m_3\psi_3 + m_{10}\psi_{10} - m_4\psi_4 - Q_A \left| 1 - \frac{T_0}{T_A} \right| \dots\dots\dots(C13)$$

$$\Delta\psi_{cm} = m_{17} (\psi_{18} - \psi_{17}) \dots\dots\dots(C14)$$

Solution heat exchanger

$$\Delta\psi_{\text{she,ht}} = m_1\psi_1 + m_5\psi_5 - m_6\psi_6 - m_2\psi_2 \dots\dots\dots(\text{C15})$$

Solution pump:

$$\Delta\psi_{\text{pump}} = m_4 (P_4 - P_5)/P_5 \dots\dots\dots(\text{C16})$$

3.4 VAPOUR COMPRESSION CYCLE ANALYSIS

Energy Balance

$$Q_{\text{con}} = m_{\text{vc}} (h_{19} - h_{20}) \dots\dots\dots(\text{D1})$$

$$Q_{\text{evap}} = m_{\text{vc}} (h_{22} - h_{21}) \dots\dots\dots(\text{D2})$$

$$Q_{\text{comp}} = m_{\text{vc}} (h_{19} - h_{22}) \dots\dots\dots(\text{D3})$$

$$S_{19} = S_{22} \dots\dots\dots(\text{D4})$$

Assume eff. of condenser evaporator heat exchanger.

$$\text{eff}_{\text{cehe}} = 0.95 \dots\dots\dots(\text{D5})$$

$$Q_{\text{con}} = Q_e / \text{eff}_{\text{cehe}} \dots\dots\dots(\text{D6})$$

Qcon is calculated by directly proportional to efficiency if base system for analysis is reversed.

$$W_{\text{comp}} = m_{\text{vc}} \times (h_{19} - h_{20}) \dots\dots\dots(\text{D7})$$

$$Q_{\text{evap}} = m_{\text{vc}} \times (h_{22} - h_{21}) \dots\dots\dots(\text{D8})$$

$$Q_{\text{con}} = m_{\text{vc}} [h_{\text{fg}20} + c_p (T_{19} - T_{20})] \dots\dots\dots(\text{D9})$$

$$c_p (T_{19} - T_{20}) = h_{19} - h_{g20} (m_{\text{vc}} = \text{const.}) \dots\dots\dots(\text{D10})$$

$$P_{21} = P_{22} \dots\dots\dots(\text{D11})$$

The results obtained directly from the simulations are the thermodynamic state and the mass and volume flow rates at every representative point in the thermodynamic cycles of the compression and absorption systems, the heat flux in each heat exchanger, the electric power required by the compressor and the pump and the compression and absorption systems performance (COP_c and COP_a) which are obtained from Eqs given below respectively. The global system performance (COP_g) is calculated as:

Compression System Performance

$$\text{COP}_c = Q_{\text{evap}} / W_{\text{comp}} \dots\dots\dots(\text{E1})$$

Absorption System Performance

$$\text{COP}_a = Q_e / (Q_g + W_{\text{pump}}) \dots\dots\dots(\text{E2})$$

Or

$$\text{COP}_a = Q_{\text{con,c}} / (Q_g + W_{\text{pump}}) \dots\dots\dots(\text{E3})$$

Global (Cascade) System Performance

$$\text{COP}_g = (Q_{\text{evap}} / (Q_g + W_{\text{comp}} + W_{\text{pump}})) \dots\dots\dots(\text{E4})$$

3.5 CASCADE SYSTEM EXERGY ANALYSIS

Table3.1: Fuel-Product-Loss Definition

SYSTEM	FUELS	PRODUCTS	LOSSES
Generator	$(E_{11}-E_{12})$	$(E_7+E_1-E_6)$	-
Evaporator Assembly	$(E_7+E_2-E_4)$	$(E_{20}-E_{19})$	$(E_{18}-E_{17})+(E_{14}-E_{13})$
Solution Pump	W_p	(E_5-E_4)	-
Solution Heat Exchanger	(E_1-E_2)	(E_6-E_5)	-
Compressor	W_c	$(E_{19}-E_{22})$	-
Expansion Valve	$(E_{20}-E_{21})$	-	-
Evaporator	$(E_{21}-E_{22})$	$[(1-(T_o/T_{evap}))Q_{evap}]$	-
Overall System	$(E_{11}-E_{12})+W_c$	$[(1-(T_o/T_{evap}))Q_{evap}]$	$(E_{14}-E_{13})+(E_{18}-E_{17})$

Table3.1: Fuel-Product-Loss Definition

TABLE 3.2: DEFINITION OF EXERGETIC TERMS

System	Exergy destruction E_D	Exergy efficiency of component $\eta_{ex,k}$	Exergy Loss E_L	Exergy Destruction Ratio Y_D	Exergy Loss Ratio Y_L
Generator	$(E_{11}-E_{12})-(E_{7}+E_{1}-E_{6})$	$(E_{7}+E_{1}-E_{6})/(E_{11}-E_{12})$		$(E_{11}-E_{12})-(E_{7}+E_{1}-E_{6})/(E_{11}-E_{12})$	
Evaporator Assembly	$(E_{7}+E_{2}-E_{4})-(E_{20}-E_{19})-(E_{18}-E_{17})-(E_{14}-E_{13})$	$(E_{20}-E_{19})/(E_{7}+E_{2}-E_{4})$	$(E_{18}-E_{17})+(E_{14}-E_{13})$	$[(E_{7}+E_{2}-E_{4})-(E_{20}-E_{19})-(E_{18}-E_{17})-(E_{14}-E_{13})]/(E_{11}-E_{12})$	$(E_{18}-E_{17}+E_{14}-E_{13})/(E_{11}-E_{12})$
Solution Pump	$W_p-(E_{5}-E_{4})$	$(E_{5}-E_{4})/W_p$		$(W_p-(E_{5}-E_{4}))/(E_{11}-E_{12})$	
Solution Heat Exchanger	$(E_{1}-E_{2})-(E_{6}-E_{5})$	$(E_{6}-E_{5})/(E_{1}-E_{2})$		$(E_{1}-E_{2})-(E_{6}-E_{5})/(E_{11}-E_{12})$	
Compressor	$W_c-(E_{19}-E_{22})$	$(E_{19}-E_{22})/W_c$		$(W_c-(E_{19}-E_{22}))/(E_{11}-E_{12})$	
Expansion valve	$E_{20}-E_{21}$			$(E_{20}-E_{21})/(E_{11}-E_{12})$	
Evaporator	$(E_{21}-E_{22})- [(1-(T_o/T_{evap}))Q_{evap}]$	$[(1-(T_o/T_{evap}))Q_{evap}]/(E_{21}-E_{22})$		$(E_{21}-E_{22})- [(1-(T_o/T_{evap}))Q_{evap}]/(E_{11}-E_{12})$	
Overall system	$(E_{11}-E_{12}+W_c)- [(1-(T_o/T_{evap}))Q_{evap}]- (E_{18}-E_{17})-(E_{14}-E_{13})$	$[(1-(T_o/T_{evap}))Q_{evap}]/(E_{11}-E_{12}+W_c)$	$(E_{18}-E_{17})+(E_{14}-E_{13})$	$[(E_{11}-E_{12}+W_c)- [(1-(T_o/T_{evap}))Q_{evap}]- (E_{18}-E_{17})-(E_{14}-E_{13})]/(E_{11}-E_{12}+W_c)$	$(E_{18}-E_{17}+E_{14}-E_{13})/(E_{11}-E_{12}+W_c)$

Table 3.2: Definition of Exergetic Terms

PARAMETRIC INVESTIGATION

Table A Operating conditions for the cascade system

<i>i</i>	$T(i)$ ($^{\circ}\text{C}$)	$h(i)$ (kJ/kg)	$S(i)$ (kJ/kg.K)	$m(i)$ (Kg/s)	$X(i)$ (% LiBr)	Exergy (kJ/kg)
1	105	257.63	2.2435	0.1707	64.0	225.889
2	77.93	194.34	2.2744	0.1707	64.0	223.551
3	58.5	194.34	2.2744	0.1707	64.0	223.551
4	47	126.74	2.2784	0.1836	59.5	227.817
5	47.74	128.186	2.2823	0.1836	59.5	227.861
6	70.2	186.90	2.4451	0.1836	59.5	229.434
7	105	2696.9	8.4482	0.0129	-	24.668
8	47	196.30	0.6632	0.0129	-	23.341
9	10	196.30	0.6632	0.0129	-	23.341
10	10	251.35	8.9053	0.0129	-	20.557
11	372	3624.34	6.3067	0.0340	-	118.908
12	200	2308.09	4.7272	0.0340	-	90.6942
13	35	308.57	6.8957	1.9887	-	0.0000
14	46	319.17	6.9309	1.9887	-	0.79358
17	35	308.57	6.8957	2.9169	-	0.0000
18	46	319.57	6.9309	2.9169	-	0.6035
19	120	1736.0	6.131	0.02311	-	13.634
20	20	293.6	1.32847	0.02311	-	2.915
21	-29.9	293.6	1.4238	0.02311	-	31.31
22	-29.9	1423.0	6.131	0.02311	-	304.65

The operating conditions of vapour absorption cycle are taken from [1].

4.1 Variation of COP of vapour compression system with Efficiency of evaporator condenser heat exchanger:

Efficiency(%)	COP_c
70	1.286
75	1.517
80	1.8
85	2.155
90	2.613
95	3.227

Table 4.1 Cascade Heat Exchanger Efficiency Vs COP_c

4.2. Variation of COP of Vapour Absorption System with Efficiency of Evaporator-Condenser Heat Exchanger:

Efficiency(%)	COP_a
70	0.742955
75	0.675698
80	0.626764
85	0.580958
90	0.542972
95	0.516158

Table 4.2 Cascade Heat Exchanger Efficiency Vs COP_a

4.3. Variation of Global COP of System with Efficiency of Evaporator- Condenser Heat Exchanger:

Efficiency (%)	COPg
70	0.315436
75	0.321056
80	0.329225
85	0.335112
90	0.341385
95	0.351168

Table 4.3 Cascade Heat Exchanger Efficiency Vs COPg

4.4 Variation of COP of Vapour Compression System with Intermediate temperature level (condensation temperature of the compression system) for evaporation temperature -30 °C :

Intermediate Temperature (°C)	COPc
15	4.158155
16	3.994854
17	3.910483
18	3.814039
19	3.743331
20	3.664291
21	3.617312
22	3.553933
23	3.485863
24	3.402164
25	3.32633

Table 4.4 Intermediate temperature Vs COPc at $T_{\text{evap}} = - 30^{\circ}\text{C}$

4.5 Variation of COP of Vapour Compression System with Intermediate temperature level (condensation temperature of the compression system) for evaporation temperature of -25 °C:

Intermediate Temperature (°C)	COPc
15	4.997618
16	4.662904
17	4.494344
18	4.390426
19	4.25978
20	4.165908
21	4.088414
22	4.022919
23	3.969573
24	3.867532
25	3.821493

Table 4.5 Intermediate temperature Vs COPc at $T_{\text{evap}} = -25^{\circ}\text{C}$

4.6 Variation of COP of Vapour Compression System with Intermediate temperature level (condensation temperature of the compression system) for evaporation temperature of -20 °C:

Intermediate Temperature [°C]	COPc
15	5.770962
16	5.299526
17	5.04298
18	4.851772
19	4.697369
20	4.585347
21	4.509893
22	4.46271
23	4.414359
24	4.387746
25	4.353827

Table 4.6 Intermediate temperature Vs COPc at $T_{\text{evap}} = -20^{\circ}\text{C}$

4.7 Variation of COP of Vapour Absorption System with Intermediate temperature level (Condensation temperature of the compression system):

Intermediate Temperature [°C]	COPa
15	0.686761
16	0.692204
17	0.695194
18	0.698774
19	0.701516
20	0.704706
21	0.706668
22	0.709397
23	0.712439
24	0.716346
25	0.720056

Table 4.7 Intermediate temperature Vs COPa

4.8 Variation of COP of Cascade System with Intermediate temperature level (condensation temperature of the compression system) for evaporation temperature -30 °C :

Intermediate Temperature [°C]	COPg
15	0.511125
16	0.50857
17	0.507177
18	0.505519
19	0.504256
20	0.502795
21	0.501901
22	0.500662
23	0.499289
24	0.497535
25	0.495882

Table 4.8 Intermediate temperature Vs COPg at $T_{\text{evap}} = - 30^{\circ}\text{C}$

4.9 Variation of COP of Cascade System with Intermediate temperature level (condensation temperature of the compression system) for evaporation temperature -25 °C :

Intermediate Temperature [°C]	COPg
15	0.521901
16	0.518018
17	0.515868
18	0.514471
19	0.512628
20	0.511242
21	0.510056
22	0.509022
23	0.508158
24	0.506447
25	0.505649

Table 4.9 Intermediate temperature Vs COPg at $T_{\text{evap}} = -25^{\circ}\text{C}$

4.10 Variation of COP of Cascade System with Intermediate temperature level (condensation temperature of the compression system) for evaporation temperature -20 °C :

Intermediate Temperature [°C]	COPg
15	0.529308
16	0.525024
17	0.522392
18	0.520268
19	0.51844
20	0.517046
21	0.516073
22	0.515449
23	0.514798
24	0.514434
25	0.513964

Table 4.10 Intermediate temperature Vs COPg at $T_{\text{evap}} = -20^{\circ}\text{C}$

4.11 EXERGETIC ANALYSIS OF CASCADE SYSTEM

System	Exergy destruction E_D	Exergy efficiency of component $\eta_{ex,k}$	Exergy Loss E_L	Exergy Destruction Ratio Y_D	Exergy Loss Ratio Y_L
Generator	7.091	0.7487		27.47	
Evaporator Assembly	29.72	-0.5254	1.397	1.054	0.04952
Solution Pump	0.1582	0.2176		0.0056	
Solution Heat Exchanger	0.765	0.7628		2.282	
Compressor	604.1	-0.9294		21.41	
Expansion valve	-28.39			-1.006	
Evaporator	-19.14	0.93		-264.3	
Overall system	594.1	-0.7448	1.397	1.741	0.0041

Table 4.11 Exergetic Analysis of Cascade System

5.1 Variation of COP of vapour compression system with Efficiency of evaporator condenser heat exchanger:

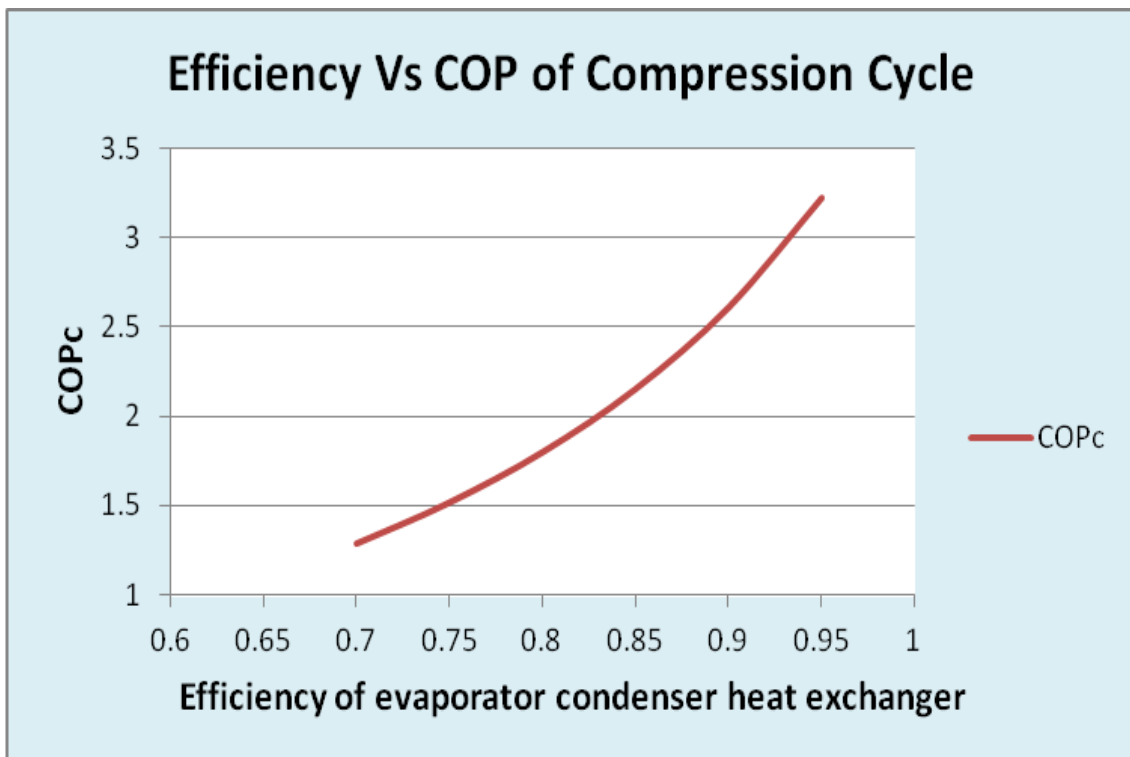


Fig 5.1 Efficiency Vs COPc

Graph shows the increasing tendency of COPc with increase in efficiency of evaporator condenser heat exchanger.

5.2. Variation of COP of Vapour Absorption System with Efficiency of Evaporator-Condenser Heat Exchanger:

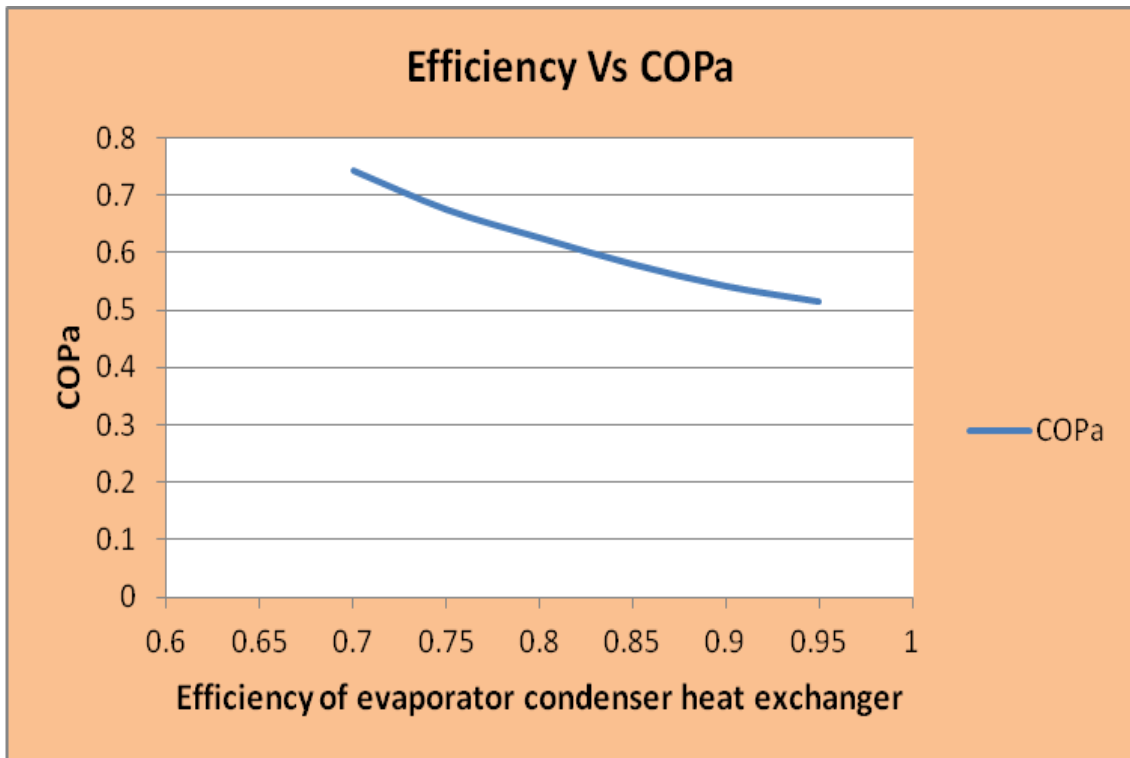


Fig 5.2 Efficiency Vs COPa

Graph shows the decreasing tendency of COPa with increase in efficiency of evaporator condenser heat exchanger.

5.3 Variation of COP of Cascade System with Efficiency of Evaporator- Condenser Heat Exchanger:

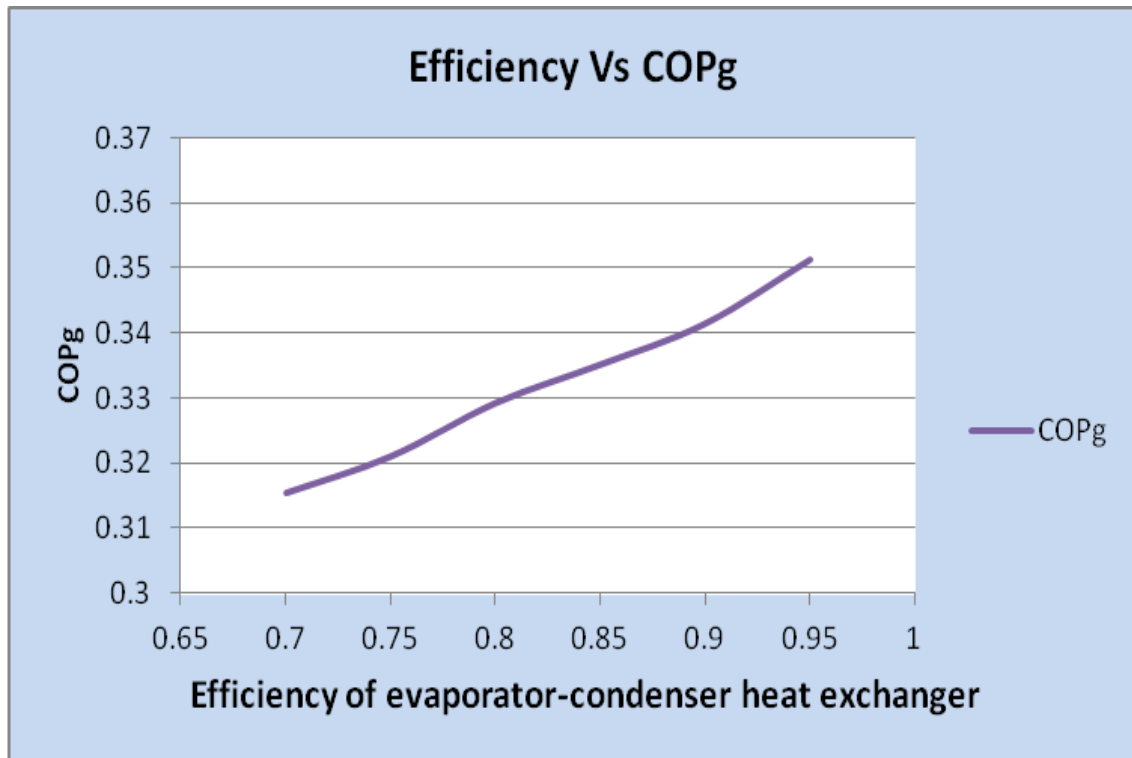


Fig 5.3 Efficiency Vs COPg

Graph shows the increasing tendency of COPg with increase in efficiency of evaporator condenser heat exchanger.

5.4 Comparison of COP of Compression system, Absorption system and Cascade system with increase of efficiency of cascade heat exchanger

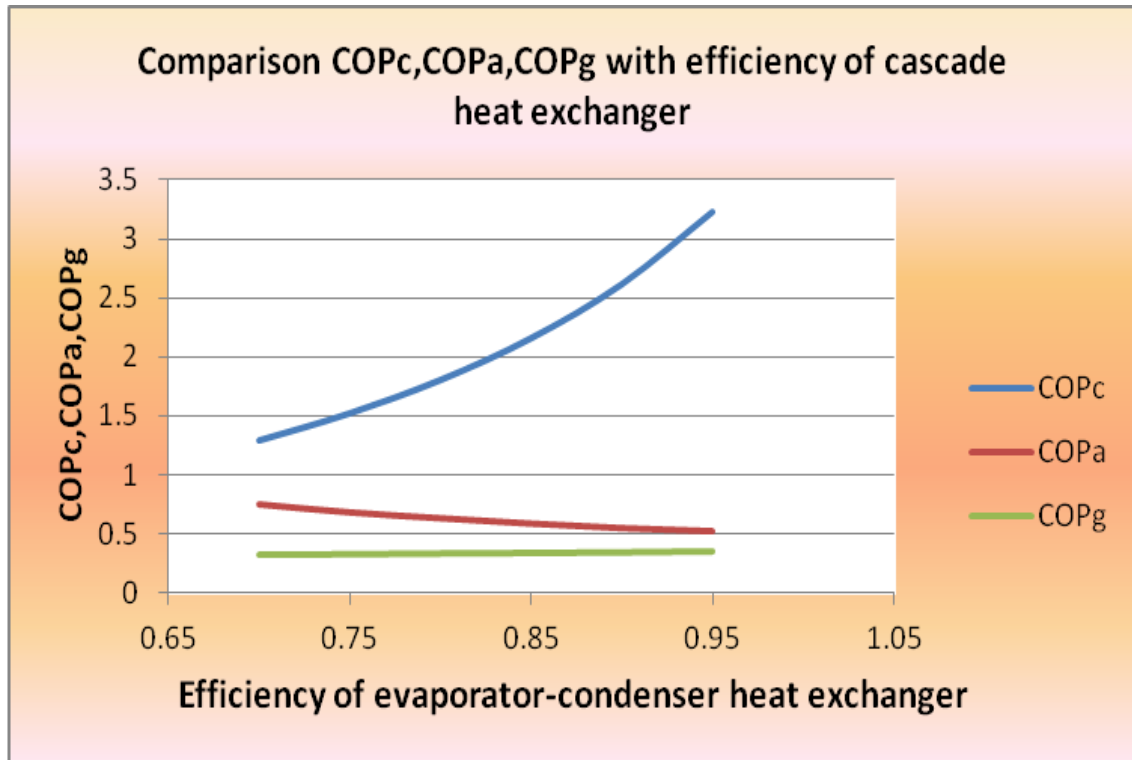


Fig.5.4 Efficiency Vs COPc, COPa, COPg

Graph shows that COP of compression system increases , but COP of absorption decreases and COP of Cascade system is slightly increase with increase in efficiency of evaporator-condenser heat exchanger.

5.5 Variation of COP of Vapour Compression System with Intermediate temperature level (condensation temperature of the compression system)for evaporation temperature of -30 °C:

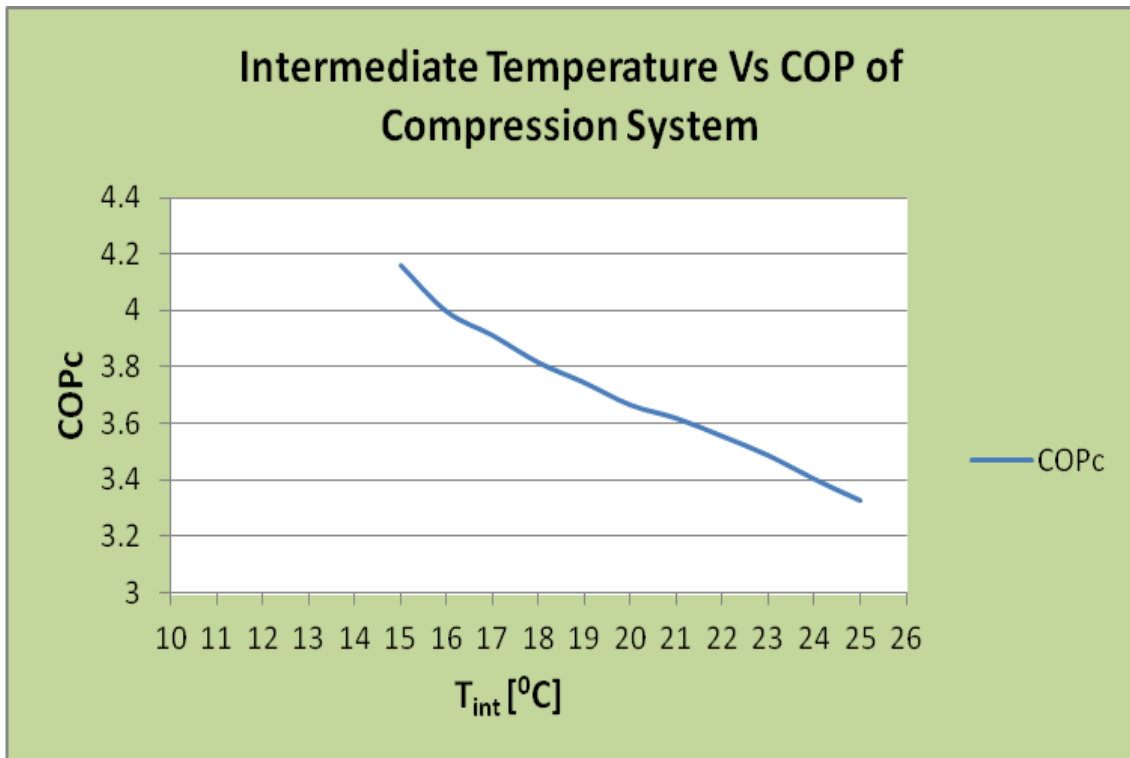


Fig5.5 Compression system COP vs intermediate temperature for evaporation temperature of -30 °C

Graph shows the COP_c decreases with increase of intermediate temperature level (Condensation Temperature of the compression system) with NH₃ as refrigerant in the compression stage and for evaporation temperature of -30 °C

5.6 Variation of COP of Vapour Compression System with Intermediate temperature level (condensation temperature of the compression system) for evaporation temperature of -25 °C:

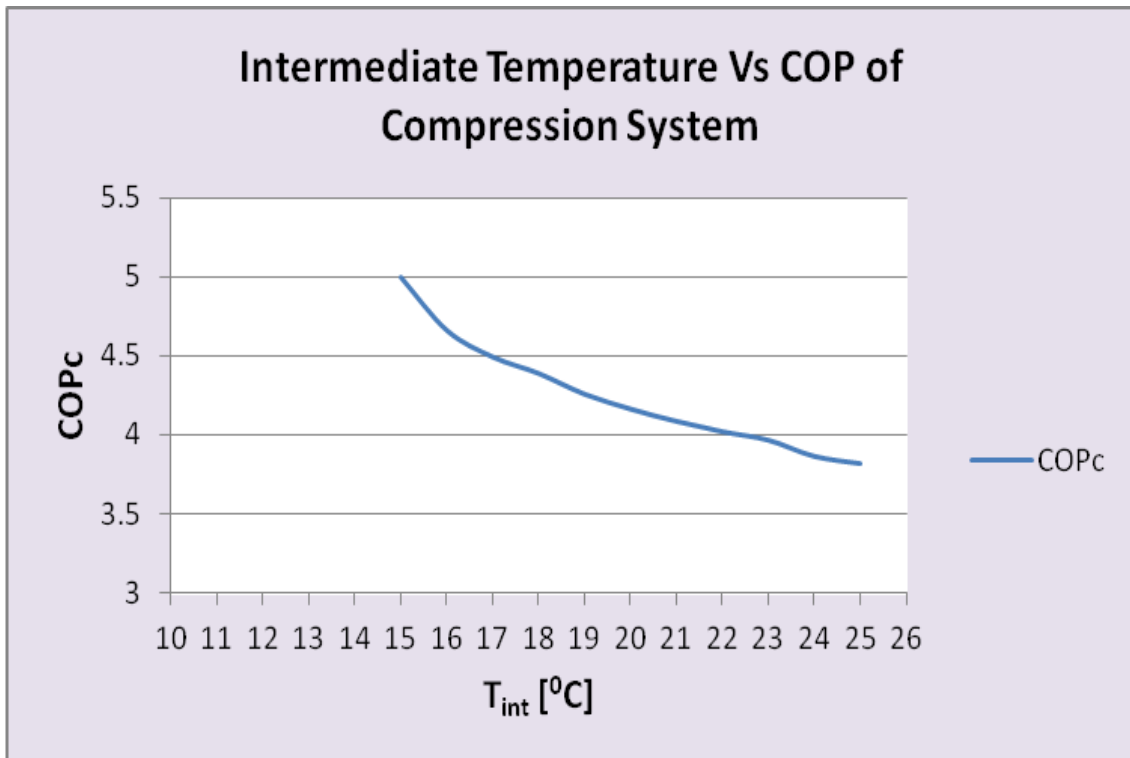


Fig5.6 Compression system COP vs intermediate temperature for evaporation temperature of -25 °C

Graph shows the COP_c decreases with increase of intermediate temperature level (Condensation Temperature of the compression system) with NH_3 as refrigerant in the compression stage and for evaporation temperature of -25 °C

5.7 Variation of COP of Vapour Compression System with Intermediate temperature level (condensation temperature of the compression system) for evaporation temperature of -20°C :

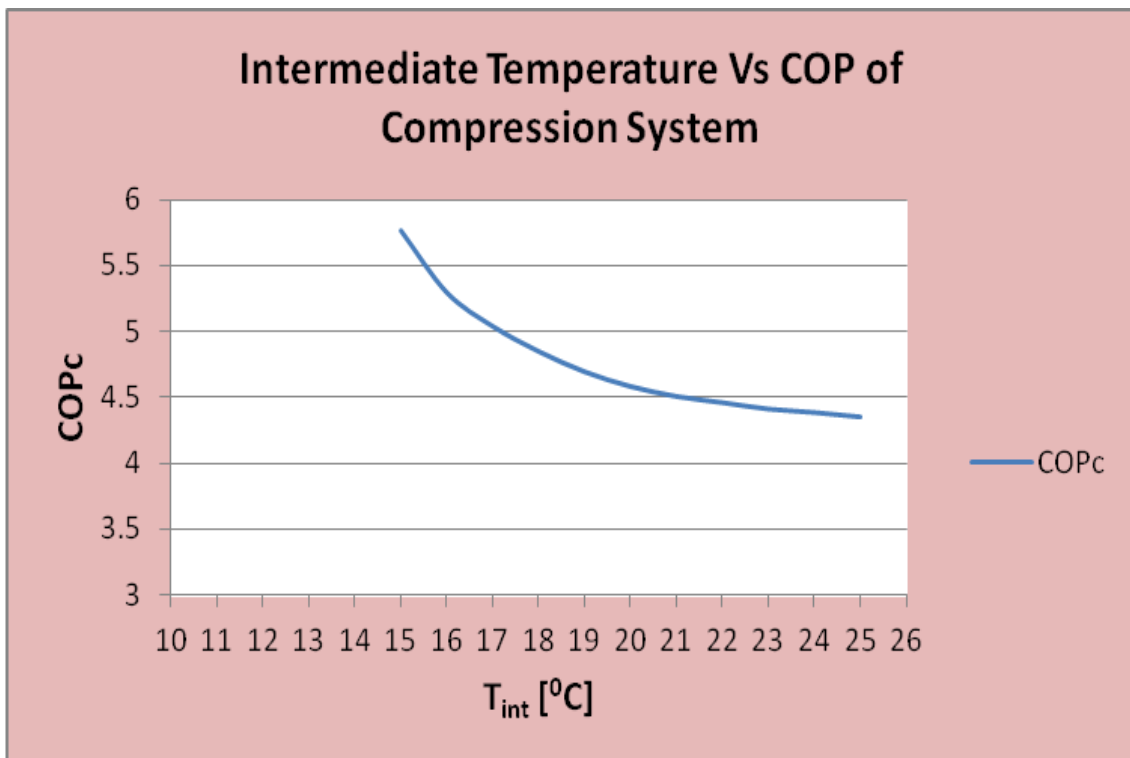


Fig5.7 Compression system COP vs intermediate temperature for evaporation temperature of -20°C

Graph shows the COP_c decreases with increase of intermediate temperature level (Condensation Temperature of the compression system) with NH_3 as refrigerant in the compression stage and for evaporation temperature of -20°C

5.8 Variation of COP of Vapor Absorption System with Intermediate temperature level (condensation temperature of the compression system):

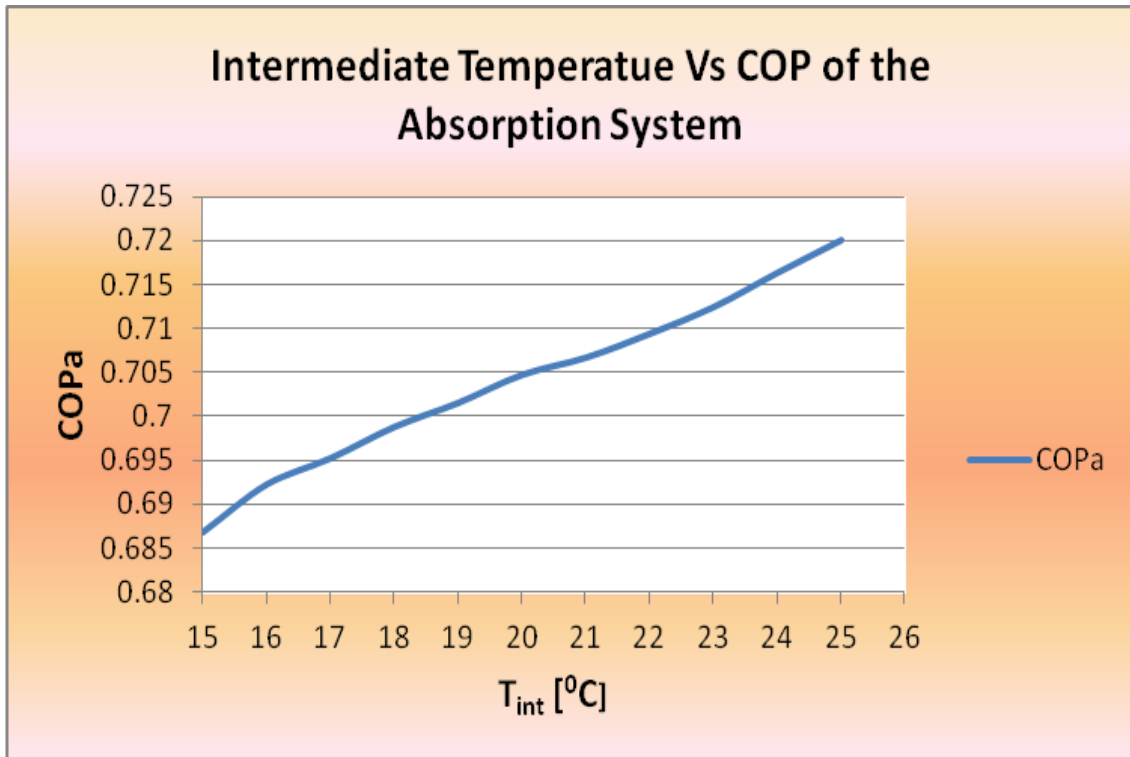


Fig.5.8 Intermediate temperature Vs COPa

Graph shows the COPa increases with increase of intermediate temperature level (Condensation Temperature of the compression system) with NH_3 as refrigerant in the compression stage

5.9 Variation of COP of Cascade System with Intermediate temperature level (condensation temperature of the compression system) for evaporation temperature of -30 °C:

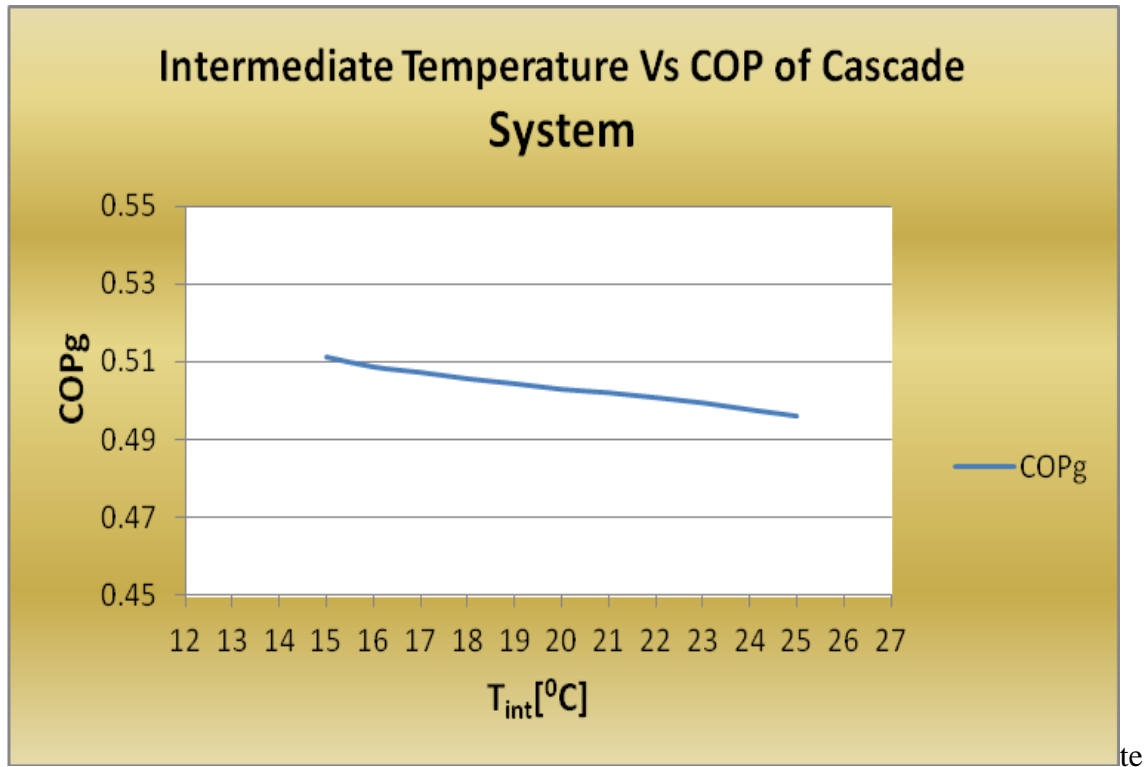


Fig5.9 Cascade system COP vs intermediate temperature for evaporation temperature of -30 °C

Graph shows the COP_g slightly decreases with increase of intermediate temperature level (Condensation Temperature of the compression system) with NH_3 as refrigerant in the compression stage and for evaporation temperature of -30 °C

5.10 Variation of COP of Cascade System with Intermediate temperature level (condensation temperature of the compression system) for evaporation temperature of -25 °C:

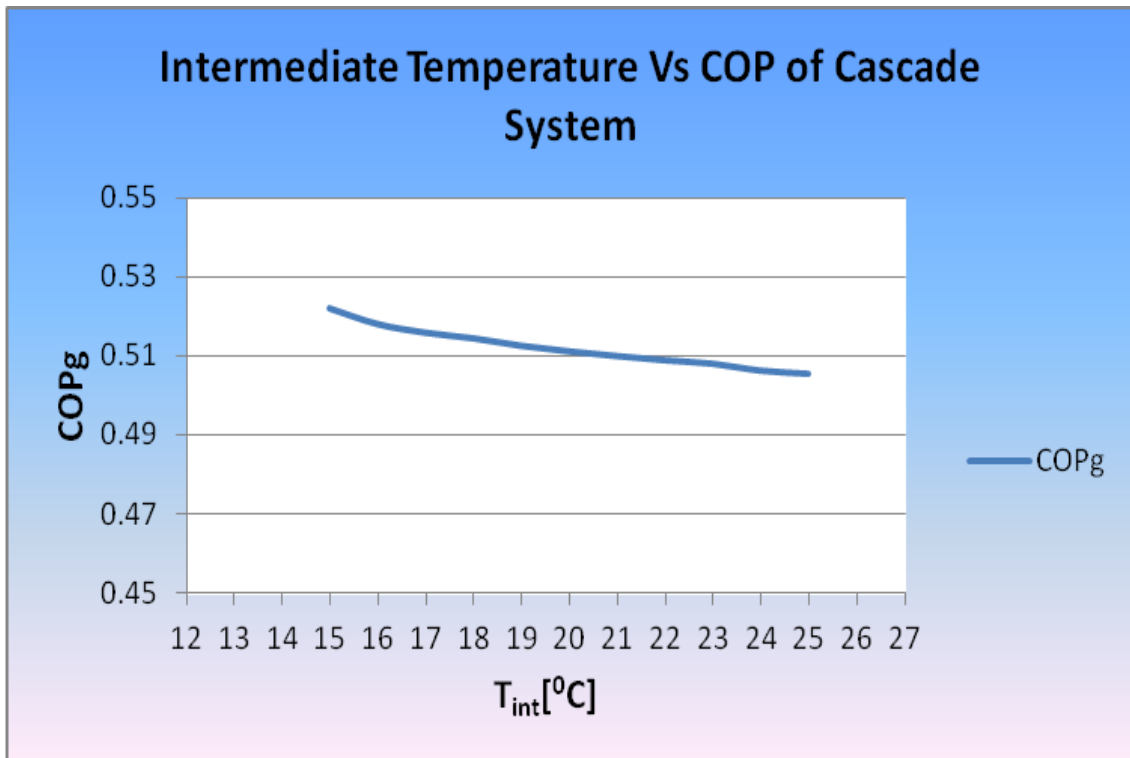


Fig5.10 Cascade system COP vs intermediate temperature for evaporation temperature of -25 °C

Graph shows the COP_g slightly decreases with increase of intermediate temperature level (Condensation Temperature of the compression system) with NH_3 as refrigerant in the compression stage and for evaporation temperature of -25 °C

5.11 Variation of COP of Cascade System with Intermediate temperature level (condensation temperature of the compression system) for evaporation temperature of -20°C :

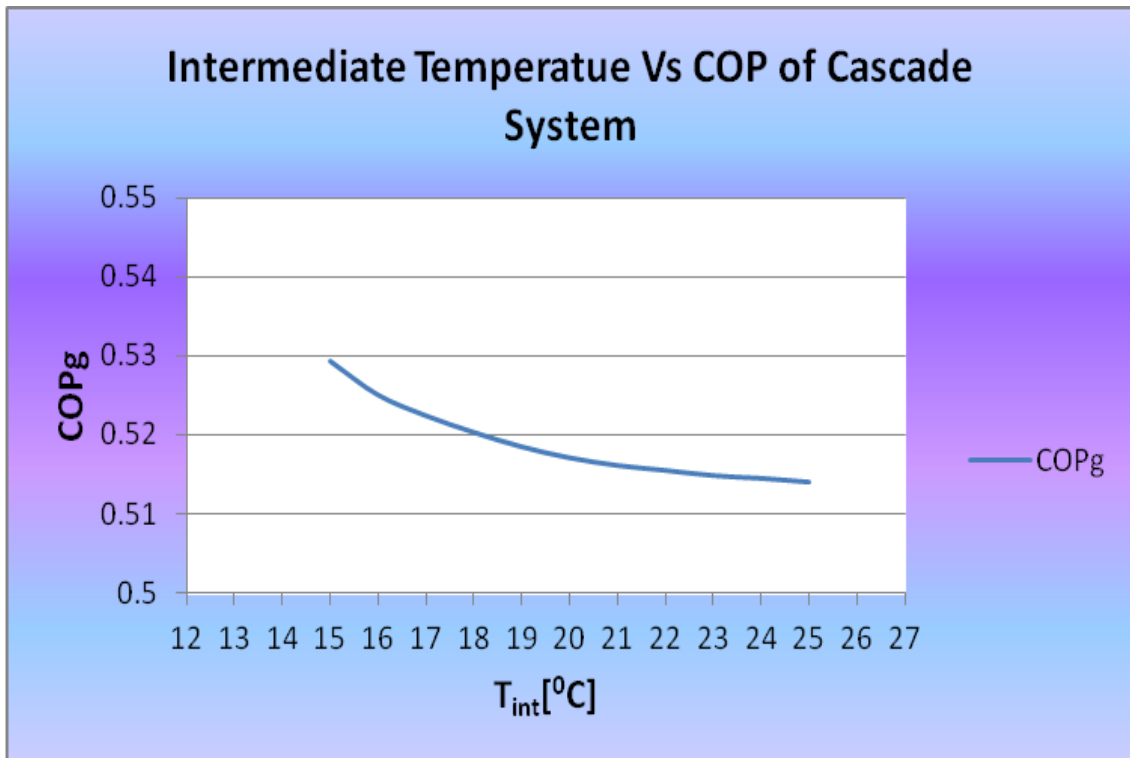


Fig5.11 Cascade system COP vs intermediate temperature for evaporation temperature of -20°C

Graph shows the COPg slightly decreases with increase of intermediate temperature level (Condensation Temperature of the compression system) with NH_3 as refrigerant in the compression stage and for evaporation temperature of -20°C

5.12 Comparison of COP of compression system at different evaporator temperature with increase in intermediate temperature

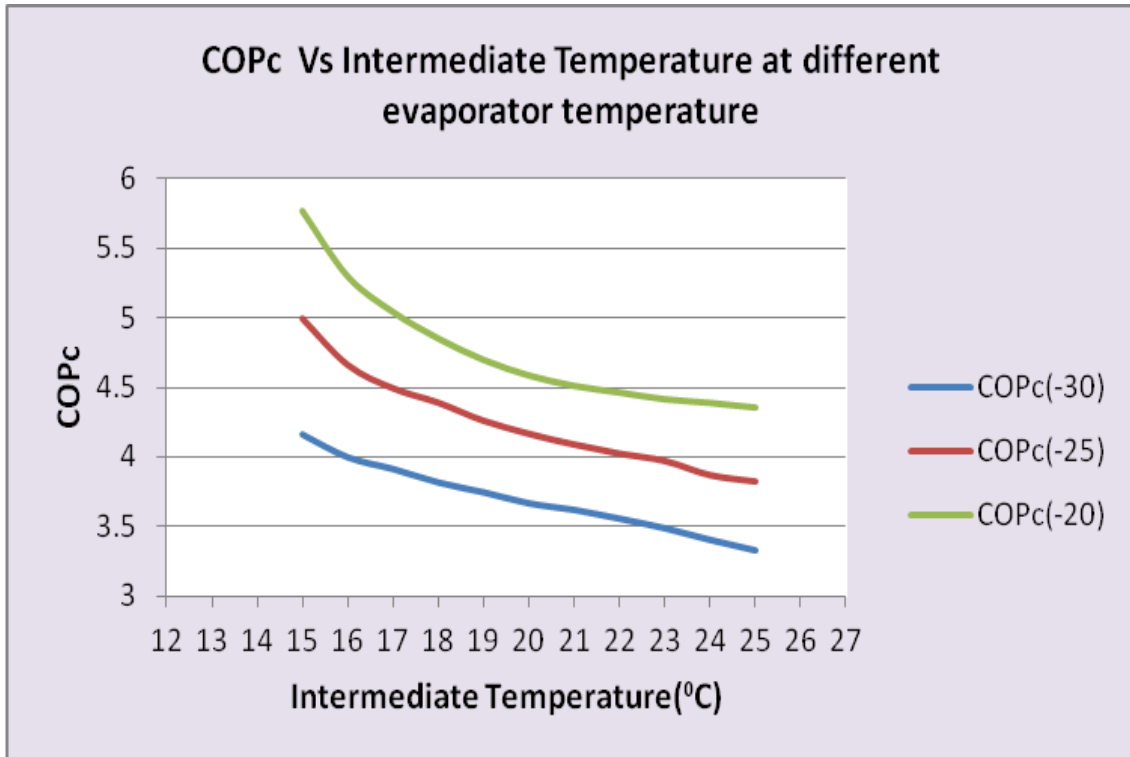


Fig.5.12 COP of compression system Vs Intermediate Temperature at different evaporator temperature

It can be noticed that the intermediate temperature increase causes simultaneously a compression COP decrease. . The compression COP decrease is less significant as the evaporation temperature decreases.

5.13 Comparison of COP of cascade system at different evaporator temperature with increase in intermediate temperature

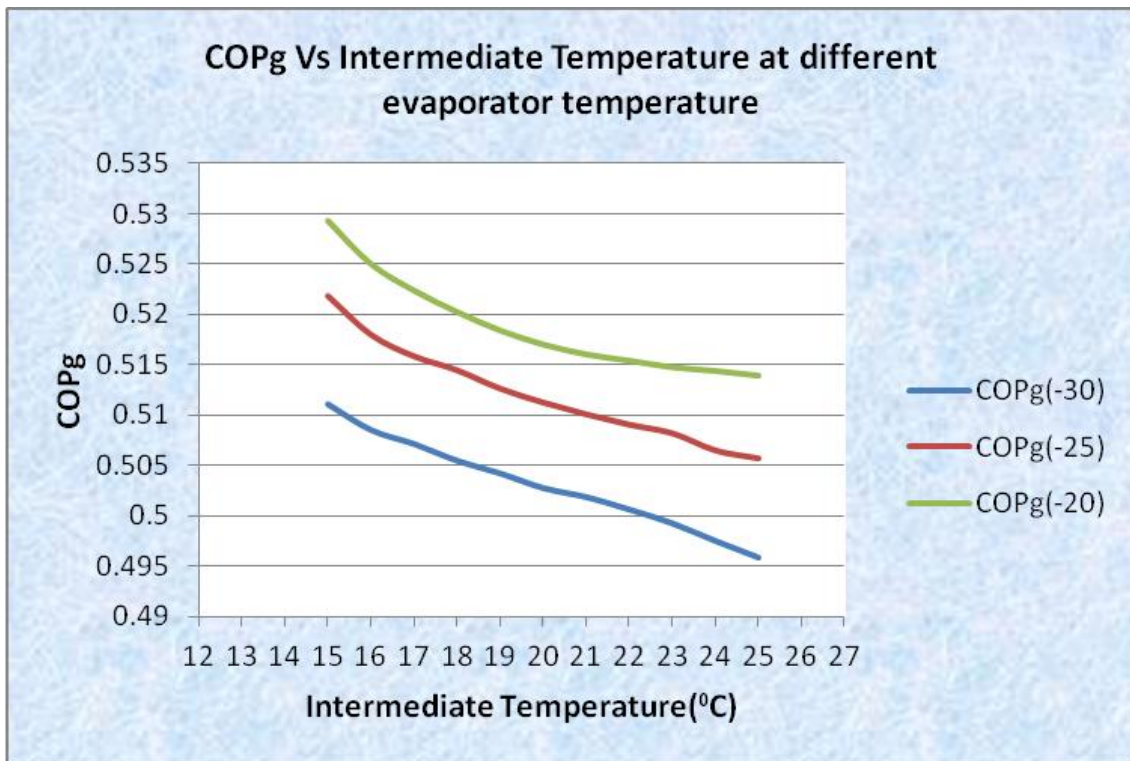


Fig.5.13 COP of cascade system Vs Intermediate Temperature at different evaporator temperature

COP of this cascade refrigeration system is decreasing with the increase in condensing temperature . and COPg also in decreasing tendency with decrease in evaporation temperature.

5.14 Compression system COP (COPc), Absorption system COP (COPa), Cascade system COP (COPg) vs intermediate temperature level (condensation temperature of the compression system) for evaporation temperature of -30, -25 and -20 °C

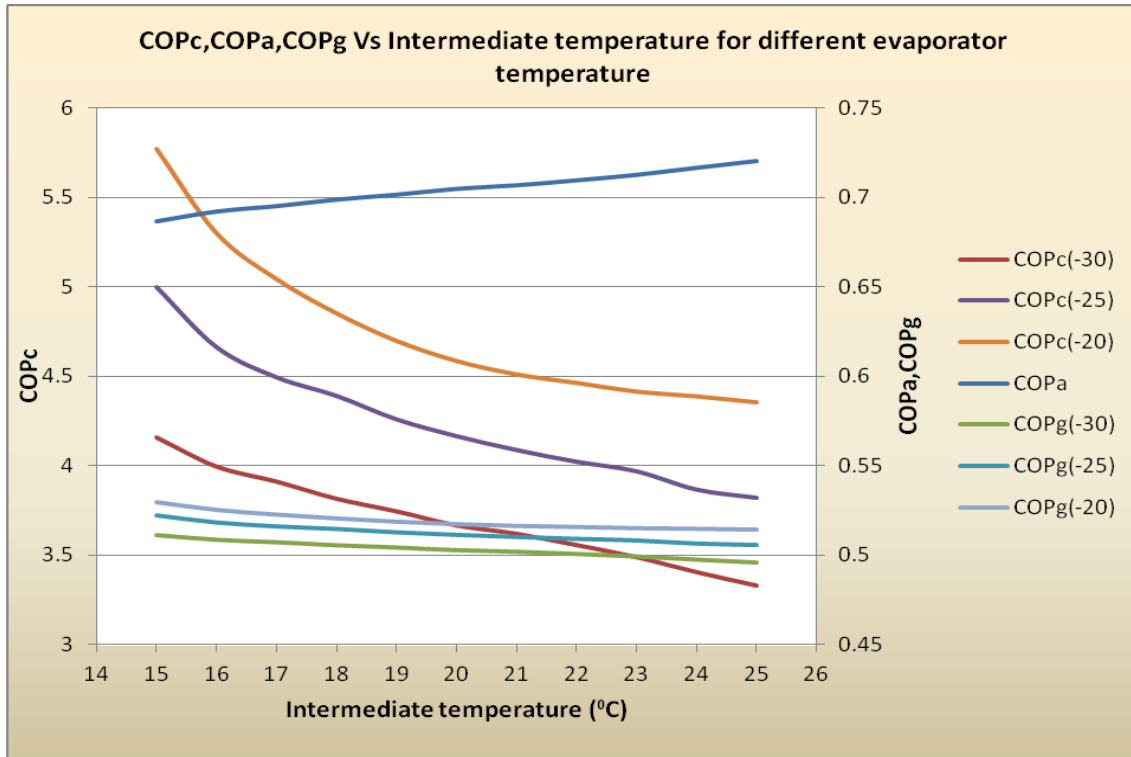


Fig 5.14. COPc, COPa & COPg VS Intermediate Temperature for different evaporator temperature

Fig 5.14. shows the results of the COP values of the compression, absorption and cascade systems with NH₃ as the refrigerant in the compression system and evaporation temperatures of -30, -25 and -20 °C obtained by varying the intermediate temperature while keeping the remaining design parameters. It can be noticed that the intermediate temperature increase causes simultaneously a compression COP decrease and an absorption COP increase. The compression COP decrease is less significant as the evaporation temperature decreases. The intermediate temperature that produces the maximum COP depends on the evaporation temperature of the compression system.

CONCLUSION AND SCOPE OF FUTURE WORK

6.1 CONCLUSION

- It has been observed that the intermediate temperature level is an important design parameter that causes an opposite effect on the COP of the compression and absorption systems. Therefore, the cascade system COP presents a maximum when the intermediate temperature is varied. Therefore, the results from the simulation model can be an outstanding tool at the system design stage.
- It can be noticed that the intermediate temperature increase causes simultaneously a compression COP decrease and an absorption COP increase. The compression COP decrease is less significant as the evaporation temperature decreases. The intermediate temperature that produces the maximum COP depends on the evaporation temperature of the compression system.
- It has been also observed that with increase in efficiency of condenser-evaporator heat exchanger, the COP of vapour absorption system decreases and vapour compression system increases; and consequently COP of Cascade system is slightly increases.

6.2 SCOPE OF FUTURE WORK

- An outstanding design parameter in cascade refrigeration systems is the intermediate temperature level at which the low temperature system gives up the condensing heat to the high temperature system. In this analysis, the intermediate temperature level is defined by the condensation temperature of the compression system. This temperature has an opposite effect on the COP values of the compression and absorption systems. Therefore, an optimum COP value can be calculated for the overall cascade system.
- To determine and evaluate the adaptability, from the viewpoint of the energetic requirements, between the refrigeration and the cogeneration systems. Moreover, the performance of the global (refrigeration–cogeneration system) can be calculated.

REFERENCES

- [1] M.M. Talbi, B. Agnew, Exergy analysis: an absorption refrigerator using lithium bromide and water as the working fluids, *Applied Thermal Engineering* 20 (2000) 619-630.
- [2] R.D. Misra , P.K. Sahoo , S. Sahoo , A. Gupta, Thermoeconomic optimization of a single effect water/LiBr vapour absorption refrigeration system, *International Journal of Refrigeration* 26 (2003) 158–169.
- [3] R.D. Misra, P.K. Sahoo, A. Gupta, Thermoeconomic evaluation and optimization of a double-effect H₂O/LiBr vapour-absorption refrigeration system, *International Journal of Refrigeration* 28 (2005) 331–343
- [4] Jose Fernandez-Seara , Jaime Sieres, Manuel Vazquez, Compression–absorption cascade refrigeration system, *Applied Thermal Engineering* 26 (2006) 502–512
- [5] Berhane H. Gebreslassie , Marc Medrano , Dieter Boer, Exergy analysis of multi-effect water–LiBr absorption systems: From half to triple effect, *Renewable Energy* 35 (2010) 1773–1782
- [6] R.D. Misra, P.K. Sahoo, A. Gupta, Thermoeconomic evaluation and optimization of an aqua-ammonia vapour-absorption refrigeration system, *International Journal of Refrigeration* 29 (2006) 47–59
- [7] B. Kundu, P.K. Mondal , S.P. Datta , S. Wongwises, Operating design conditions of a solar-powered vapor absorption cooling system with an absorber plate having different profiles: An analytical study, *International Communications in Heat and Mass Transfer* 37 (2010) 1238–1245
- [8] Yuyuan Wu, Yan Chen, Tiehui Wu, Experimental researches on characteristics of vapor–liquid equilibrium of NH₃–H₂O–LiBr system, *International Journal of Refrigeration* 29 (2006) 328–335

- [9] A. Kilicarslan, An experimental investigation of a different type vapor compression cascade refrigeration system, *Applied Thermal Engineering* 24 (2004) 2611–2626.
- [10] Paul Kalinowski, Yunho Hwang, Reinhard Radermacher, Saleh Al Hashimi, Peter Rodgers, Application of waste heat powered absorption refrigeration system to the LNG recovery process, *international journal of refrigeration* 32 (2009) 687– 694.
- [11] Jaime Sieres, Jose Fernandez-Seara, Evaluation of the column components size on the vapour enrichment and system performance in small power NH₃–H₂O absorption refrigeration machines, *International Journal of Refrigeration* 29 (2006) 579–588.
- [12] I. Horuza , T.M.S. Callander, Experimental investigation of a vapor absorption refrigeration system, *International Journal of Refrigeration* 27 (2004) 10–16.
- [13] S. Arivazhagan , R. Saravanan , S. Renganarayanan, Experimental studies on HFC based two-stage half effect vapour absorption cooling system, *Applied Thermal Engineering* 26 (2006) 1455–1462.
- [14] Shenyi Wu, Ian W. Eames, Innovations in vapour-absorption cycles, *Applied Energy* 66 (2000) 251-266.
- [15] Guo-liang Ding, Recent developments in simulation techniques for vapour-compression refrigeration systems, *International Journal of Refrigeration* 30 (2007) 1119-1133
- [16] Jin-Soo Kim, Felix Ziegler , Huen Lee, Simulation of the compressor-assisted triple-effect H₂O/LiBr absorption cooling cycles, *Applied Thermal Engineering* 22 (2002) 295–308.
- [17] Y. Kaita, Simulation results of triple-effect absorption cycles, *International Journal of Refrigeration* 25 (2002) 999–1007.

[18] Tzong-Shing Lee, Cheng-Hao Liu, Tung-Wei Chen, Thermodynamic analysis of optimal condensing temperature of cascade-condenser in CO₂/NH₃ cascade refrigeration systems, *International Journal of Refrigeration* 29 (2006) 1100-1108.

[19] J. Alberto Dopazo, Jose Fernandez-Seara , Jaime Sieres, Francisco J. Ufia, Theoretical analysis of a CO₂-NH₃ cascade refrigeration system for cooling applications at low temperatures, *Applied Thermal Engineering* 29 (2009) 1577–1583